Project Acronym/ Acronimo del progetto:

INTEGRIDS

Project title:

Electric and thermal grids integration with energy flexible building

Titolo del progetto:

Studio dell'integrazione di reti elettriche e termiche con la flessibilità energetica degli edifici

Deliverable name	Modello e power flow della rete
Deliverable N°.	D4.3
Task	T4.3
Authors: Approved:	Grazia Barchi, Mattia Secchi David Moser
Due date	30/08/2019

efre · fesr Südtirol · Alto Adige
Europäischer Fonds für regionale Entwicklung
Fondo europeo di sviluppo regionale
EUROPEAN UNION
AUTONOME PROVINZ BOZEN SÜDTIROL
PROVINCIA AUTONOMA DI BOLZANO ALTO ADIGE

Table of contents

Executive summary

The increasing penetration of distributed renewable thermal and electrical energy generation and the need of decarbonizing the existing energy infrastructure (both thermal and electrical) has led to a new set of challenges. These will have to be tackled in the next 10 years to make sure that the full potential of renewables can be exploited within electric grids and thermal networks.

INTEGRIDS will explore the concept of integrated energy grids defined as the synergy between thermal and electrical grids to enable high renewable energy penetration in efficient energy buildings and districts.

In previous reports of work package 4 the emphasis was at a regional and national level, thus the energy flow and the renewable integration at transmission level were taken into consideration.

In this report the focus is on the distribution grid and the detailed model and analysis provided by power flow solutions. The aim is to evaluate the impact of photovoltaic generation on a medium voltage distribution grid introducing renewable sources, battery storage and/or electric vehicles to mitigate their impact.

In the first part of the document, the model of the grid, its components and the classic steady state power flow are summarized based on the literature. After that, a series of tool used for power system model and analysis are reported. In the end, OpenDSS was chosen as the candidate software for the simulation in this task.

Due to the variability and time dependency of RES, especially PV generators, it is most suitable to perform a sort of "dynamic" power flow analysis in order to characterize the impact on a specific grid. The performed simulations are more correctly named quasi-steady state analysis because they consider their dependence with time (until 1 sec of resolution) but do not consider the dynamic events connected to the electrical transient (< 1 μs).

With this respect a dedicated software has been developed and tested on a medium voltage test grid (i.e. IEEE 37 bus).

The results show that:

1. If the loads and PV systems are one-phase balanced or three-phase, OpenDSS shows no significant difference in the infractions along the 3 phases;
2. The steady state simulations show a situation which is highly unrealistic, since the loads consumption and PV production are not constant during the day;
3. Thus, QSS simulations are needed to isolate the parts of the grid which are highly influenced by the presence of loads and PV systems;
4. The most distant buses have the highest number of infractions regarding voltage
5. The main feeders of the grid, joining the side branches to the transformer are the most susceptible of overloading;
6. A small PV penetration, around 10-15%, helps in reducing the undervoltages to zero, while producing little overvoltage issues. Even an extremely high PV penetration (such as 90%) just produces 9% overvoltage infractions during a year;

7. The transformer is also experiencing overloads, due to excesses of both generation and consumption, so particular care has to be placed in sizing the PV system;
8. PHEVs produce a sizeable increase in undervoltages because of the concentration of the charging in a part of the day where PV is not producing;
9. Thus, the mitigation with EVs is not very effective, V2G ("vehicle to grid") or V2H ("vehicle to home") algorithms could improve the results;
10. Batteries are by far the best mitigation technique since they prove to be effective both in terms of over and undervoltages.

1 Introduction and context

The electricity grid is actively evolving due to the high penetration of renewable energy sources, the proliferation of non-linear loads (such as the electric vehicle) and the transformation of final consumers also to producers (i.e., prosumers).

The traditional electricity grid, usually characterized by one-directional power flows and centralized power plant, is changing in a more complex system where traditional monitoring and control are not effective, and the capability to host new generation and loads can create some issues to the system.

The power grid purpose is to provide electricity to various types of customers (such as domestic, commercial, or industrial). From centralized power plants, the system transmits and distributes the electricity demand to the final users. A representation of this infrastructure in Figure 1.

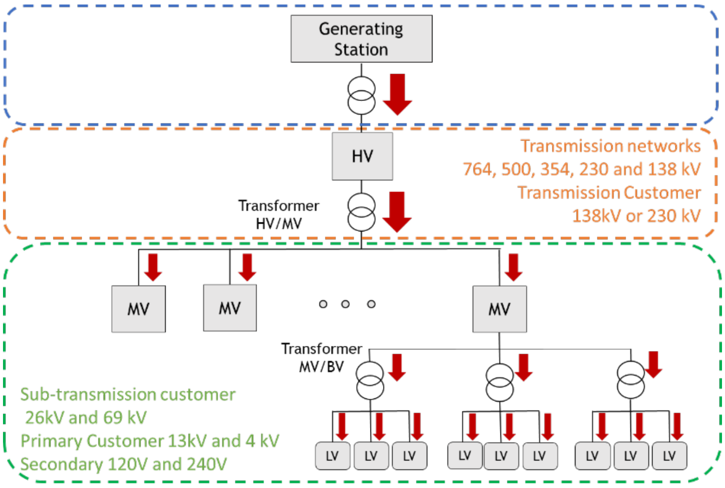

Figure 1 - Simplified diagram of the electricity system

The transmission system, usually also referred to as a primary system, connects the significant commercial and industrial customers who require high voltage supply. On the other hand, the distribution systems work at lower voltages and connect the small commercial, small industrial and all most domestic customers. When we focus only at the neighbourhood's level, we refer to the low voltage system.

Nowadays, the traditional and passive grid is becoming smart to guarantee the proper operability and reliability even in the presence of distributed generation or dispersed loads. For this reason, it is always more common to refer to the electricity system evolution as a paradigm change called "smart grid" (SG).

The main characteristic of SG is to integrate the classic electromechanical physical structure with the information and communication infrastructure (ICT) which can enable advanced measurements, monitoring and control techniques. The new structure can allow the grid to manage the two-way flow of electric power and data, which gives the possibility to enhance the grid response and automate grid operations. The improvement in grid management favours the inclusion of DG and renewable energy, reducing CO2 emissions. The principal differences between the traditional grid and the smart grid are presented in [1] and summarized below.

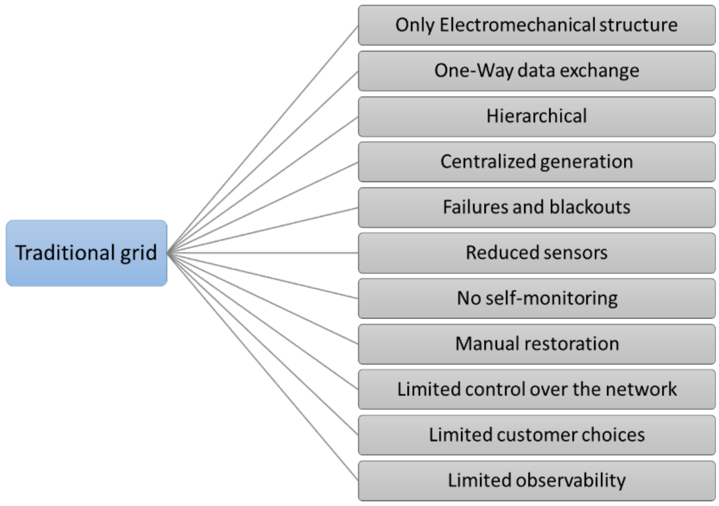

(a)

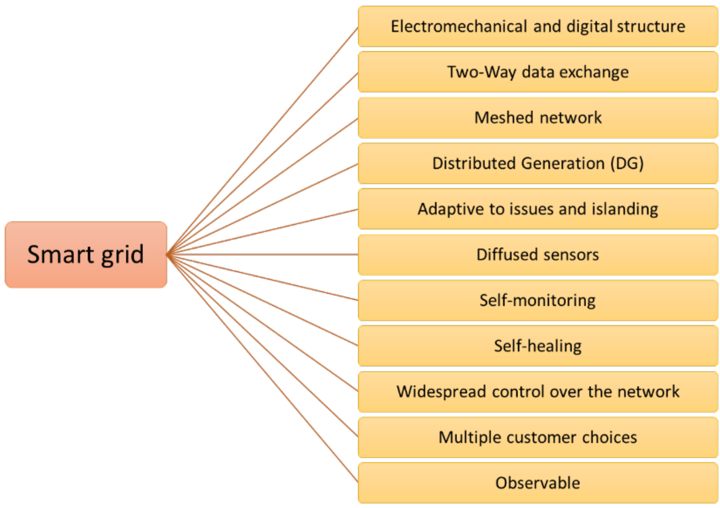

(b)

Figure 2 - Features of the traditional and smart grid [1]

The adoption technology, methodology and regulations typically of smart grid, have the aim to totally or partially solve some challenges for example:

- Intermittent generation (e.g. solar and wind plant which depends on the variable natural source)
- Integration of energy storages (useful to reduce the variability of solar or wind power plant)
- Transmission system planning
- Cost for installation and site identification for large/medium generators
- …

2 Objective and structure of the report

In the previous reports (i.e. D4.1 and D4.2) we analyse the impact of renewable and transients at transmission level with energy flows and optimization methodology.

In this report, conversely, we focus on the analysis of distribution level where most of DG is connected.

Specifically, this report aims to present the power flow analysis for distribution grid using three-phase modelling for both steady-state and dynamic behaviour. Even in the literature for dynamic analysis it is commonly mean the electromagnetic or transient events, in this report we refer to dynamic power flow when we consider the inclusion of distributed generation or variable loads (such as photovoltaic, energy storage, electric vehicle, …) where the behaviour is strongly dependent from the time and the season.

After presenting the classic theory behind the power flow analysis, a section will be dedicated to software for power system analysis, highlighting the similarities and differences and justifying the use of OpenDSS tool. A brief introduction of the OpenDSS is then given.

In the second part of the report, methodology and results of the use of OpenDSS considering the PV, energy storage and EV penetration are shown to quantify the benefits of the power flow analysis to quantify the impact of DG at distribution grid.

3 Distribution systems

Radial distribution feeder is characterized by only one path of power flow from the source (distribution substation) to each customer. A typically distribution system will be composed of one or more distribution substations consisting of one or more feeders.

Components of the feeder consist of the following:

- Three phases primary main feeder
- Three phases, two-phase, and single-phase
- Step-type voltage regulator
- In-line transformers
- Shunt capacitor banks
- Distribution transformer
- Secondaries
- Three-phase, two-phase, single-phase load.

The distribution system is usually unbalanced due to the variety of loads to be served. Moreover, the space between conductor and the resistance and reactance characteristic is different and for this purpose, power flow and short-circuit algorithm for transmission systems are not adequate.

In order to perform a distribution feeder analysis, it is important to have a map of the feeder. Specifically, it is required to have the following information:

Lines (overhead and underground)	– Where – Distance – Details (conductor size, phasing)
Distribution information	– Location – KVA rating – Phase connection
In-line transformer	– Location – KVA rating – Connection
Shunt capacitor	– Location – KVar rating – Phase connection
Voltage regulator	– Location – Phase connection – Type (single-phase or three-phase)
Switches	– Location – Normal open/close status

4 Distribution grid modelling theory

In this chapter the most common elements of the grid will be described, paying attention to their modelling and how it is performed in the software used for the simulations. The descriptions are based on "Distribution System Modelling and Analysis" by William H.Kersting [2].

4.1 Lines model

4.1.1 Detailed 3-phase Line Model

The distribution feeders are usually modelled with simplified versions of a detailed 3-phase line model, which can be seen in Figure 4. The line is connecting nodes "n" and "m" and consists of three phases (a,b and c), where the most notable parameters are the line to ground voltage of each line and the admittance of the grounding before and after the line (Y_{abc}).

The line losses are represented by a resistance and an inductance, which are then summed up by the line impedances (Z_{aa}, Z_{bb}, Z_{cc}). Z_{ab}, Z_{ca} and Z_{bc} are the lines to line impedances.

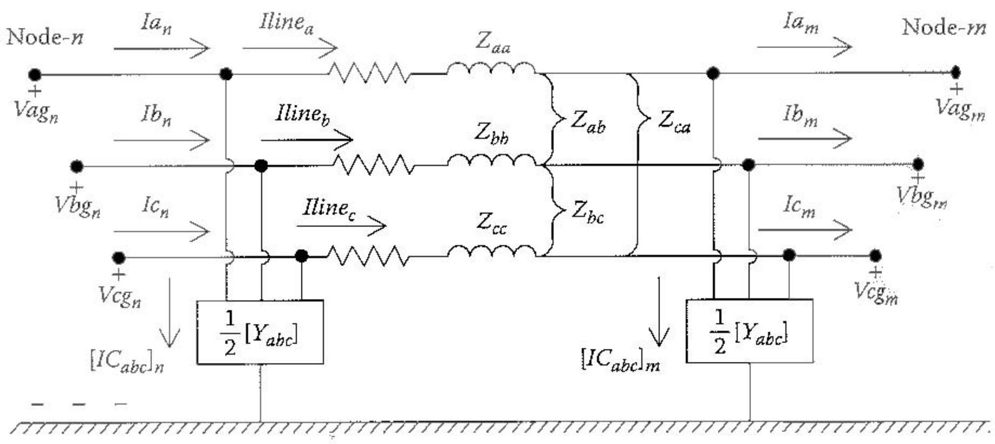

Figure 3 - 3-Phase electric line detailed model [2]

The most important relation is the *forward step* equation, where the output at node m is estimated as a function of the input at node n

$$\begin{bmatrix} \mathbf{V_{LG,abc}} \\ \mathbf{I_{abc}} \end{bmatrix}_n = \begin{bmatrix} \mathbf{a} & \mathbf{b} \\ \mathbf{c} & \mathbf{d} \end{bmatrix} \cdot \begin{bmatrix} \mathbf{V_{LG,abc}} \\ \mathbf{I_{abc}} \end{bmatrix}_m \tag{1}$$

Where a,b,c and d are matrices which depend on constant parameters of the line such as the impedance or the admittance. When we need to perform the *backwards step*, the equation must be reversed

$$\begin{bmatrix} \mathbf{V_{LG,abc}} \\ \mathbf{I_{abc}} \end{bmatrix}_m = \begin{bmatrix} \mathbf{d} & -\mathbf{b} \\ -\mathbf{c} & \mathbf{a} \end{bmatrix} \cdot \begin{bmatrix} \mathbf{V_{LG,abc}} \\ \mathbf{I_{abc}} \end{bmatrix}_n \tag{2}$$

Going back to the voltage equations and solving for $V_{LG,abc,m}$ as a function of $V_{LG,abc,n}$ we get again, a relationship involving constant elements a and b

$$\mathbf{V_{LG,abc,m}} = \begin{bmatrix} \mathbf{a^{-1}} & \mathbf{a^{-1}b} \end{bmatrix} \cdot \begin{bmatrix} \mathbf{V_{LG,abc}} \\ \mathbf{I_{abc}} \end{bmatrix}_n \tag{3}$$

The LL voltages are then obtained by difference

$$\begin{bmatrix} V_{ab} \\ V_{bc} \\ V_{ca} \end{bmatrix}_m = \begin{bmatrix} 1 & -1 & 0 \\ 0 & 1 & -1 \\ -1 & 0 & 1 \end{bmatrix} \cdot \begin{bmatrix} V_{ag} \\ V_{bg} \\ V_{cg} \end{bmatrix}_m \tag{4}$$

4.1.2 Simplified Model: Two-Port

A simplified version of the detailed model with lumped parameters is the two-port model, which can be seen in Figure 5. Vs and Zs are the voltage and impedance of the source, Z0 is the impedance of the line and ZL is the impedance of the load.

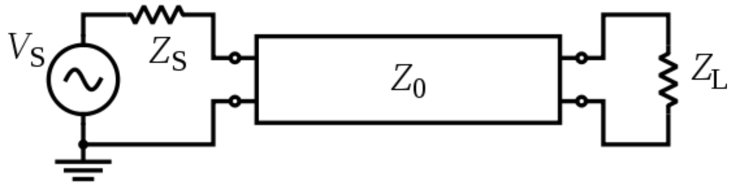

Figure 4 - Two-Port model for a transmission line

The electrical line is modelled by considering its characteristic impedance Z_0. The lower the impedance, the higher the power which is absorbed by the load (Z_L) and the lower the losses along the line. The importance of this model lies in the possibility to describe the losses as a function of one parameter only, Z_0, which is the ratio of the complex voltage to the complex current at any point along the line, provided the impedance of the generator Z_s is small enough to be discarded

$$Z_0 = \frac{V_s \underline{/\theta_s}}{I_0 \underline{/\theta_0}} = Z_0 \underline{/\theta_s - \theta_0} \tag{5}$$

When the lines are short and the propagation delays are negligible, the transmission cable can be approximated as a series impedance (R+iX) followed by a shunt admittance. Usually, the shunt admittance is halved and placed at the two ends of the circuit, forming a *pi-section*

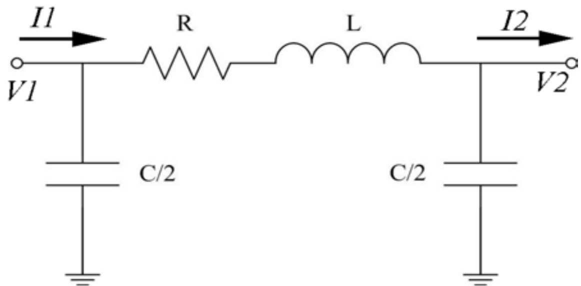

Figure 5 - Pi-section model for a transmission line

where the sending voltage V_1 is equal to

$$V_1 = \left(V_2 \cdot \frac{Y}{2} + I_2\right) \cdot Z + V_2 \tag{6}$$

and the Y is the admittance matrix of the circuit.

4.2 Loads

Loads can be modelled in several ways, each of them assuming a particular parameter is known:

1. Apparent Power (kVAs) and Power Factor (PF)
2. Real Power (kW) and Power Factor (PF)

3. Real Power (kW) and Reactive Power (kVAr)

However, all of them require the voltage level to be known in order to determine the current consumption of the load. Since the voltage is normally unknown at $t = 0$, the general process involves making a guess, then iterating and estimating the current, checking if the total power is stable at the input level, then if the tolerance is respected moving on with the next iteration.

Different models can be used to represent the loads, each of them is declined differently based on the connection, Wye or Delta (see Figure 7). Note: if Delta connected, the load rated power should be expressed as LL; if Wye connected, LN or LG.

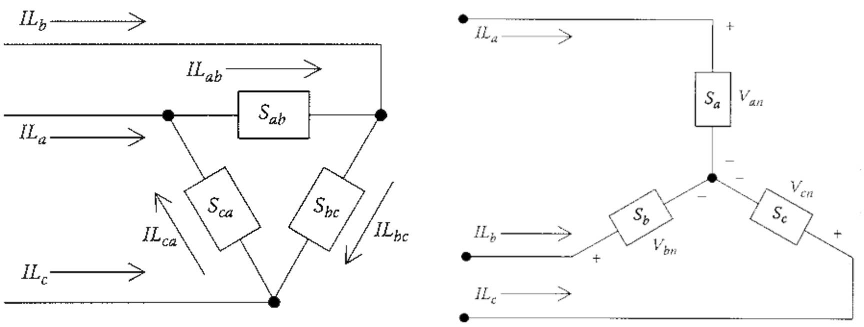

Figure 6 - Delta and Wye connected load [2]

4.2.1 Constant PQ

For the Delta connection, let consider the *ab* branch from figure 7 is examined to simplify the problem, but the same equations can be applied to the bc and ca ones. The apparent power $S_{ab}\underline{/\theta_{ab}}$ is held constant at the rated level along each branch while the LN voltages change during every iteration. If the LN voltage is $V_{ab}\underline{/\delta_{ab}}$, from the general equation of apparent power for branch ab we get

$$\mathbf{S_{ab}} = \mathbf{V_{ab}} \cdot \mathbf{I^*_{ab}} \tag{7}$$

we solve for $\mathbf{I_{ab}}$

$$\mathbf{I_{ab}} = \left(\frac{\mathbf{S_{ab}}}{\mathbf{V_{ab}}}\right)^* = \left(\frac{S_{ab}}{V_{ab}} \cdot e^{i(\theta_{ab}-\delta_{ab})}\right)^* = \frac{S_{ab}}{V_{ab}}\underline{/\delta_{ab} - \theta_{ab}} \tag{8}$$

When we consider wye connection, for the branch a, we have that the apparent power $S_a\underline{/\theta_a}$ is held constant, while the LN voltage $V_{an}\underline{/\delta_a}$ changes at each iteration. Solving for the line current yields

$$\mathbf{I_a} = \left(\frac{\mathbf{S_a}}{\mathbf{V_{an}}}\right)^* = \frac{S_a}{V_{an}}\underline{/\delta_a - \theta_a} \tag{9}$$

4.2.2 Constant Impedance

In Delta connection the apparent power is specified as input, while the LN voltages are assumed for the first iteration. An equivalent impedance $Z\underline{/\theta}$ is estimated, with the same phase angle as the apparent power, and is held constant as the voltage levels change:

$$\mathbf{Z_{ab}} = Z_{ab}\underline{/\theta_{ab}} = \frac{V^2_{ab}}{S^*_{ab}} = \frac{V^2_{ab}}{S_{ab}}\underline{/\theta_{ab}} \tag{10}$$

Solving for the current yields

$$\mathbf{I_{ab}} = \frac{\mathbf{V_{ab}}}{\mathbf{Z_{ab}}} = \frac{V_{ab}}{Z_{ab}} \underline{/\delta_{ab} - \theta_{ab}} \tag{11}$$

In Wye connection, for first step we calculate the impedance

$$\mathbf{Z_a} = Z_a \underline{/\theta_a} = \frac{V_{an}^2}{S_a^*} = \frac{V_{an}^2}{S_a} \underline{/\theta_a} \tag{12}$$

Solving for the current yields

$$\mathbf{I_a} = \frac{\mathbf{V_{an}}}{\mathbf{Z_a}} = \frac{V_{an}}{Z_a} \underline{/\delta_a - \theta_a} \tag{13}$$

4.2.3 Constant Current

The principle is the same as the constant PQ model, but this time, the currents are held constant while the voltage phase angle δ changes for each iteration. This keeps the PF of the load constant.

Delta Connection:

$$\mathbf{I_{ab}} = I \underline{/\delta_{ab} - \theta_{ab}} \tag{14}$$

Wye Connection:

$$\mathbf{I_{ab}} = I_a \underline{/\delta_a - \theta_a} \tag{15}$$

5 Power flow (load-flow) analysis

Power Flow analysis is a methodology to obtain the magnitude and phase angles of the voltage at each bus and the real and reactive power flowing in each line. The system is assumed to reach a steady state at each timestep. Nowadays the importance of power flow analysis is increasing due to the widespread diffusion of distributed energy resources, locally modifying the daily voltage and current profiles at the bus they are connected to.

Even assuming that all the load demands are known, and the generation exactly matches the consumption, some mismatch will still persist because of the line losses. For this reason, a generator bus is usually chosen as the *slack bus* without specifying its real power. It is assumed that the generator connected to this bus will assure the required real power balance.

The main steps to solve the power flow problem are:

a. Grid analysis based on the node (i.e. KCL) method
b. Selection of known and unknown bus variables depending on bus types
c. Construction of a system of nonlinear equations
d. Iterative solution of the nonlinear system using ad-hoc techniques (e.g. Gauss-Seidel or Newton- Rapson)

The power flow problem is quite simple if we consider a simplified scheme (see Figure 8). We know the total power injected or extracted from buses 1 and 2 and we want to calculate the voltage magnitudes and phase angles for each bus and the current magnitudes and phases for each line. The grid is described by the relationship between the currents at each branch and the voltages at each bus and the connection between them is the admittance matrix Y. The main benefit of having a matrix representation of the problems is the possibility of using iterative algorithms to solve the power flow.

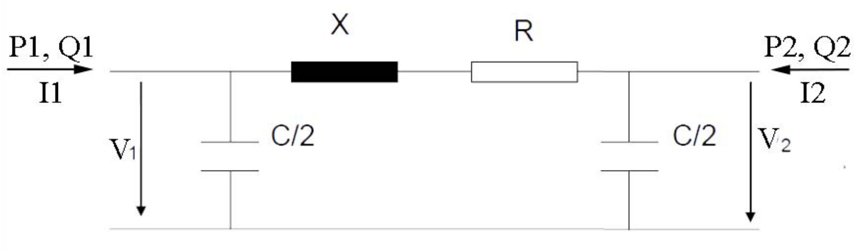

Figure 7 - Simplified scheme for a power flow analysis

The defining parameters of the electric circuit are the voltage phasors at the two ends (V_1 and V_2), the line impedance (Z_L), line admittance Y_1 and the phase difference between P and Q (ϕ).

$$\mathbf{V_1} = V_1 \underline{/\delta_1} \tag{16}$$

$$\mathbf{V_2} = V_2 \underline{/\delta_2} \tag{17}$$

$$\mathbf{Y_1} = j\omega\frac{C}{2} \tag{18}$$

$$\mathbf{Z_L} = R + iX = Z_L \underline{/\phi} \tag{19}$$

From the definition of complex power $\mathbf{S} = V \cdot I^*$ we can mathematically obtain a set of 4 equations with 8 unknowns (P_1, P_2, Q_1, Q_2, V_1, V_2, δ_1 and δ_2):

$$P_1 = \frac{V_1^2}{|Z_L|}\cos(\phi) - \frac{V_1 V_2}{|Z_L|}\cos(\phi + \delta_1 - \delta_2) \tag{20}$$

$$P_2 = \frac{V_2^2}{|Z_L|}\cos(\phi) - \frac{V_1 V_2}{|Z_L|}\cos(\phi + \delta_2 - \delta_1) \tag{21}$$

$$Q_1 = -\mathbf{Y_1} \cdot V_1^2 + \frac{V_1^2}{|Z_L|}\sin(\phi) - \frac{V_1 V_2}{|Z_L|}\sin(\phi + \delta_1 - \delta_2) \tag{22}$$

$$Q_2 = -\mathbf{Y_1} \cdot V_2^2 + \frac{V_2^2}{|Z_L|}\sin(\phi) - \frac{V_1 V_2}{|Z_L|}\sin(\phi + \delta_2 - \delta_1) \tag{23}$$

In order to solve the system at least one *slack bus* is needed, where the voltage angle and magnitude are known and serve as a reference for the others, which can be *PQ* or *PV* buses. PQ buses have an assigned value of P and Q, whereas in PV buses P and V are known.

The assumption of a reference bus which represents the connection point of the system we are analysing to the electricity grid allows us to reduce the number of unknowns from 8 to 4, allowing for an iterative algorithm application (Newton-Rhapson, Gauss-Siedel).

The first step is to compute the forward and backwards sweep matrices for all of the elements of the circuit, namely the infinite bus (considered as a balanced 12.47 kV LL source), the transformer (delta-grounded wye from 12.47 to 4.16 kV LL) and the unbalanced load (750 kVA PF=0.85, 900 kVA PF=0.9 and 1100 kVA PF=0.95).

Once the matrices are computed and the 3 phases of the load are defined, the required LV load voltage should be computed and stored as the benchmark for the iterative process to converge under a certain tolerance.

The input parameters are the line currents at both ends of the circuit and the starting voltage, which are all set at zero. The algorithm then performs several iterations while a control is performed to check if the difference between the computed voltage is close enough to the previous iteration value.

When the difference between the values at iteration i and i-1 is a small percentage of the nominal load voltage and becomes less than the tolerance the cycle stops, and the output values are saved. Figure 9 summarizes the algorithm.

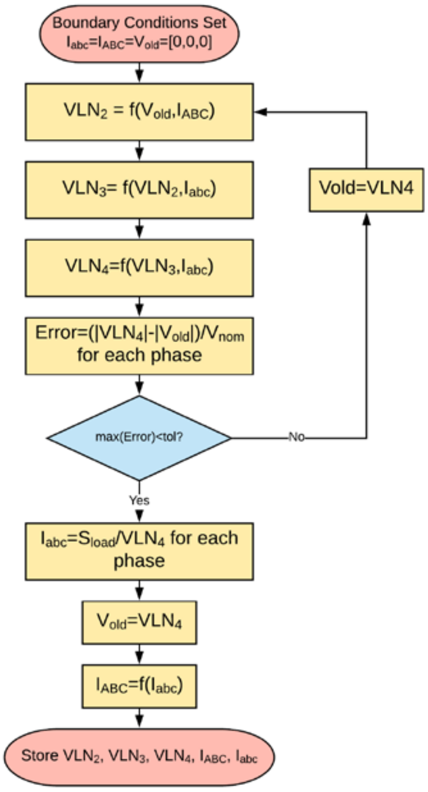

Figure 8 - Flow chart of the algorithm

6 Software and tools for power system modelling and analysis

In recent years, the inclusion of new actors in the energy and power systems has lead researcher and engineers to extend or to develop tools for simulation and analysis with more accurate models. In it always essential to remark that not a single software or model could be appropriate for everything but the choice and use of it, is strictly dependent to the question and the purpose which we would like to achieve. An interesting and complete review of modelling tools for energy and electricity systems is reported in [3]. In this paper, the authors consider 75 models (from which 71 validated) and divide the models/tool into four different categories according to the specific aim which is: power system analysis tools, operation decision support, Investment decision support and scenario. In Integrids, we worked both on Scenario simulations (in T4.1 and T4.2) using two of the tools also mentioned in [3] for this kind of analysis and in power system analysis in the present report. In order to explain the choice and use of the software applied in the following paragraph, we would like to report in a table some the tools/models (commercial or freeware) currently used by professionals or the scientific community for power system analysis. The summary and considerations are mainly based on the work performed in [3] with the integration of some additional references (i.e. [4], [5], [6]) and personal experience.

Table 1 presents the list of models/tools for power system analysis, reported in [3]. Here only the software related to this domain is isolated, for the tools regarding scenario, operation decision support and investment decision support the reader can refer directly to the paper. Three additional tools have been included in this table due to the personal experience of the researcher.

A proper tools choice should be driven by the need of modelers, it is crucial to identify a series of features and characteristics, but also the limitation of each model. In terms of approach it is important to highlight that all the software listed in Table 1 are based on a bottom-up model that means to use detailed technological descriptions for the electricity systems. Conversely, the bottom-up approach, the models can be based on the top-down approach which considers the macro-economic relationship and long-term changes [7].

Different tools are also based on a different methodology which for the context of energy/electricity system can be classified in simulations, optimizations or equilibrium. The software summarized in Table 1 are mainly based on simulation methodology, only two of them are different and they are the GridLAB-D, which use the agent-based modelling and the PyPSA which use the linear optimization. The tools/models for scenario development or operation decisions usually tend to optimize a specific function (minimize or maximize) related to cost, emissions or efficiency. On the other hand, the equilibrium methodology is commonly adopted for the energy market models which cover a different group of tools. Indeed, for example it is not restrictive to mention that the power system analysis software in Table 1 are limitations in the evaluation of costs, so the possibility to implement also the market behaviour or to evaluate the pollution emissions. However, most of them can perform optimal power flow which is commonly also associated with the generator cost.

From the technological point of view, we notice that most of the software in table 1 are able to perform detailed power flow analysis, integrate models (with different accuracy levels) of renewable energy and some of them also of energy storage (battery – BESS) or different depending on the tools. For conventional generator, except for GridLAB- D able to model only the diesel generator and for RAPSim which are not able at least at the model to include generator, the other tools can implement any power source.

The more interesting features, from our point of view, reported are: the time and spatial resolution, the presence of demand response and availability. The last characteristic to consider is the dependability from other software. There are PyPSA and PandaPower which are the library of Python, while Matpower/MOST and PSAT which can be used with Matlab, the other tools are stand-alone.

Taking into consideration all these aspects, we decide to use OpenDSS as power system analysis tools in Integrids for the current task. In the next section we describe the reason for this choice and the main characteristic of the software.

Table 1 – Characteristics of power system analysis tools from [3] with a small extension.

Tool	Temporal resolution	Spatial resolution	RES	Storage	Grid	DR	Costs	Free Software
CASPOC [8]	User-defined	Local/Single system	All	All	Power Electronics & Circuit modelling	NO	NO	NO
CYME [9]	User-defined	Single-System/Local/Regional	All	BESS	Detailed Power Simulation	NO	NO	NO
PowerFactory [10]	No limitations	Power Systems	All	Generic	Detailed Power Flow	NO	NO	NO
GridLAB-D [11]	Sub-seconds – Years	Local – National	Wind, solar	BESS	Detailed Power Flow	Yes	NO	YES
HYPERSIM [12]	10 µs	Single-System/Local/Regional	All	BESS	Detailed Power Simulation	NO	NO	YES
IPSA 2 [13]	From 30 minutes to milliseconds	Power Systems	All	All	Detailed Power Flow	Yes	NO	YES
MATPOWER/ MOST [14]	User-defined	Power Systems	All	All (Generic)	Detailed Power Flow/Scheduling (MOST)	Yes	YES	YES
OpenDSS [15]	User-defined	Balanced and unbalanced distribution feeder(s)/distribution planning area	Solar PV; All generic	All (Generic)	Full Multiphase AC Load Flow; Dynamics	Yes	NO	YES
PandaPower [6]		Balanced distribution feeder(s)/distribution planning	Solar and wind	No	AC Power Flow		YES	YES
PyPSA [5]	Hourly	National (Generic)	All	All (Generic)	Non-linear/ Linear Power Flow, NTC	Yes	YES	YES
PSAT [16]	User-defined	Power Systems	All	All	Power flow/Dynamics	Yes	YES	YES
RAPSim [17]	Minutes	Local	WP, SP	None	Detailed Power Flow	NO	NO	YES
SIMPOW [18]	Milliseconds	Single Project/Technology, Building, Island/Community & Local	All	None	Detailed Power Flow	NO	NO	NO

7 OpenDSS software engine

In Integrids the aim is to model and analyse the impact of distributed generation (e.g. photovoltaic) but also electric vehicle, heat pump or electric storage at distribution grid. Indeed, the spatial resolution is limited to district, city or maximum region but, at least in terms of power flow analysis we do not consider the transmission system. For the high voltage system, energy flow analysis has been performed in the previous task.

Concerning this, we have the aim to choose a software able to model in detail the distribution feeders as well as to track the variability of renewable generation or non-linear loads, such as electric vehicle and heat pump. Moreover, the freeware availability is also considered. The chosen software has been OpenDSS also considering the preliminary experience of some of the researchers.

OpenDSS is a comprehensive electrical power system simulation tool primarily built for electric utility power distribution systems. It is an open-source software developed by the Electric Power Research Institute (EPRI) to perform steady-state quasi steady-state and dynamic analysis in almost all the frequency domain for power distribution systems. As mentioned in the web-page [15], the software also has the growing potential to improve and perform new types of analyses regarding the smart grid, the issues of grid modernization and to help researchers study the integration of renewables, as its original function was the study of DG interconnection planning, including harmonics analysis.

Some examples of DSS applications are [15]:

- Losses, impedance, and circulating currents in unusual transformer bank configurations;
- Transformer frequency response analysis;
- Distribution automation control algorithm assessment;
- Development of DG models for the IEEE Radial test Feeders
- High-frequency harmonics and inter-harmonic interference;
- DG impact on local transmission;
- DG impact on switched capacitors and voltage regulators (e.g. wind farms)

Regarding the characteristics identified in Table 1 it is important to remark some features of OpenDSS which will be used in the next sections dedicated to simulation analysis. First, OpenDSS allow describing the multi-phase AC system considering unbalance conditions. It is true that mainly in North America than in Europe there is the diffusion of unbalance distribution system infrastructure, but it is also true that unbalance situations can also happen in European network during operational mode depending on load and generation behaviour. To track these changes, it is important to perform a more accurate power flow analysis which is called quasi-steady-state or "dynamic" power flow which takes into account the time variability over a certain period (e.g. one day, one month, one year) of loads, generation or storages. This kind of analysis can help the researcher to identify when the grid can suffer from overload or overproduction and what kind of countermeasures can be adopted. Next section will give more emphasis to this point with the demonstration through simulations.

OpenDSS also has an accurate model of PV system which considers as input not only the I-V curve, but also the solar irradiance and module temperature and the inverter efficiency. A generic model of storage which can integrate not only battery system but also different kind of systems is also included in the software. Finally, even not used in this project, OpenDSS allows to perform short circuit and fault and harmonic analysis. The fault analysis can be particularly useful to identify possible problem caused by photovoltaic and inverter transient.

8 Simulation methodology

The analysis was performed initially in steady state, with the loads modelled as power conversion elements at the nominal power and the PV systems as generators producing at their maximum power point (MPP).

The simulation was then repeated in QSS for these two cases. Subsequently electric vehicles were introduced, and the simulation was repeated with and without PV systems.

At last, the batteries were introduced and all the QSS simulations previously introduced were repeated with storage.

8.1 Grid Topology

Figure shows the topology of the grid which was used for the simulations.

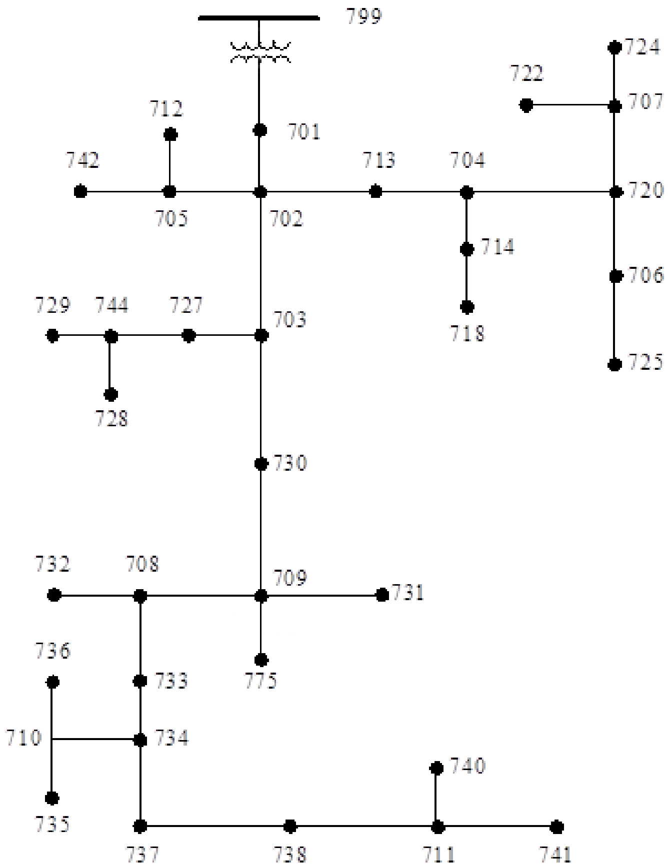

Figure 9 - Grid topology

The source bus (230 kV, 1.05 p.u.) is linked to bus 799, while the transformer joins bus 799 and 701, which is a three phase 230 to 4.8 kV Delta-Delta ungrounded machine. The rated power is 2.5 MVA.

There are 35 underground lines and 37 buses, which could be considered as the secondary cabinets of the grid, where the voltage is then lowered from 4.8 kV to 415 V, which is the distribution level.

The IEEE 37 buses grid was created as a test case for unbalanced systems, QSS simulations show at times convergence problems. For this reason, the standard IEEE grid was modified:

1. the loads were rebalanced, keeping the same apparent power nominal consumption at each bus
2. time varying profiles were created and associated to each load for QSS simulations. The peak power does not exceed the nominal load value.
3. the loop and switches of the 37 BUS grid were eliminated

8.2 Loads

All the loads are Delta Connected, as we can see from the following table. The nominal powers range from 19 to 210 kW and 9 to 105 kVAr, yet still they are all three-phase balanced loads, to ensure the convergence of the algorithm. All the loads are modelled as with the constant PQ model.

Table 2 - Voltage and loads of the IEEE 37 bus network

Buses	Phases	Conn.	V (kV)	P (kW)	Q (kVAr)
701	3	Delta	4.8	210	105
701	3	Delta	4.8	210	105
701	3	Delta	4.8	210	105
712	3	Delta	4.8	85	40
713	3	Delta	4.8	85	40
714	3	Delta	4.8	19	9
714	3	Delta	4.8	19	9
718	3	Delta	4.8	85	40
720	3	Delta	4.8	85	40
722	3	Delta	4.8	80	40
722	3	Delta	4.8	80	40
724	3	Delta	4.8	42	21
725	3	Delta	4.8	42	21
727	3	Delta	4.8	42	21
728	3	Delta	4.8	126	63
729	3	Delta	4.8	42	21
730	3	Delta	4.8	85	40
731	3	Delta	4.8	85	40
732	3	Delta	4.8	42	21
733	3	Delta	4.8	85	40

734	3	Delta	4.8	42	21
735	3	Delta	4.8	85	40
736	3	Delta	4.8	42	21
737	3	Delta	4.8	140	70
738	3	Delta	4.8	126	62
740	3	Delta	4.8	85	40
741	3	Delta	4.8	42	21
742	3	Delta	4.8	46	22
742	3	Delta	4.8	46	22
744	3	Delta	4.8	42	21

8.3 PV Systems

Then the analysis was performed by introducing PV panels in static mode, so each of them is contributing with their MPP power (power output @ STC). The following table summarizes the panels involved.

Table 3 - Nominal power of PV systems for each bus

Bus	**kV**	**Pmpp (10% Pen)**	**Pmpp (50% Pen)**	**Pmpp (90% Pen)**
701	4.8	27	135	243
712	4.8	9	45	81
713	4.8	9	45	81
714	4.8	18	90	162
718	4.8	9	45	81
720	4.8	9	45	81
722	4.8	18	90	162
724	4.8	9	45	81
725	4.8	9	45	81
727	4.8	9	45	81
728	4.8	9	45	81
729	4.8	9	45	81
730	4.8	9	45	81
731	4.8	9	45	81
732	4.8	9	45	81
733	4.8	9	45	81
734	4.8	9	45	81
735	4.8	9	45	81
736	4.8	9	45	81
737	4.8	9	45	81
738	4.8	9	45	81
740	4.8	9	45	81

741	4.8	9	45	81
742	4.8	18	90	162
744	4.8	9	45	81

The PV penetration on the grid is calculated as the total MPP power of the panels over the total nominal apparent power of the loads

$$Pen_{PV} = \frac{\sum_{i}^{N\_PV} P_{mpp,PV,i}}{\sqrt{\sum_{i=1}^{N\_LOADS}({P_i}^2 + {Q_i}^2)}} \tag{27}$$

For the sake of simplicity, we assumed there is a PV system for every load on the grid, so the equation can be written as a function of the unitary PV power value P_{PV} and the loads number

$$Pen_{PV} = \frac{P_{PV} \cdot N_{loads}}{\sqrt{\sum_{i=1}^{N_{loads}}(P_i\hat{}2 + Q_i\hat{}2)}} \tag{28}$$

Since a single bus has more than one load, the unitary PV power on each bus will be multiplied by the number of loads on each bus

$$Pen_{PV} = \frac{\boldsymbol{P_{PV}} \cdot \boldsymbol{N_{loads}}}{\sqrt{\sum_{i=1}^{N_{loads}}({P_i}^2 + {Q_i}^2)}} \tag{29}$$

Where

$$\boldsymbol{P_{PV}} = [P_{PV,Bus1} \quad \cdots \quad P_{PV,Bus37}] \tag{30}$$

$$\boldsymbol{N\_LOADS} = \begin{vmatrix} N\_LOADS_{Bus1} \\ \cdots \\ N\_LOADS_{Bus37} \end{vmatrix} \tag{31}$$

The PV power to install on every bus is finally a function of the penetration, the grid topology and the total apparent power consumption on the grid.

$$\boldsymbol{P_{PV}} = \frac{Pen_{PV} \cdot \sqrt{\sum_{i=1}^{N_{loads}}({P_i}^2 + {Q_i}^2)}}{\boldsymbol{N_{loads}}} \tag{32}$$

The PV systems are all Delta connected with a 4.8 kV LL voltage (277 V LN). The inverters are supposed to rephase the voltage to only produce active power (PF=1) and their rated power is 15% more than the MPP of the panels.

The MPP power was calculated by setting increasing values of PV penetration, ranging from 10 to 90%, in order to assess the impact of the DERs on the grid.

The inverters have a rated power of 15% more than then MPP but in all the QSS scenarios this addition is not needed because the panels never produce their maximum power rating.

The irradiance and temperature profiles were measured with a minute time resolution at the airport of Bozen in 2017 and were then scaled to obtain 15 minutes measurements.

8.4 Electric Vehicles Load Profiles

The EV profiles were generated synthetically with the free software developed by Grahn and Munkhammar [19] which employs a Markov chain to generate activity patterns. The chosen absorption power is 3.5 kW, the standard charging load of a plug-in hybrid electric vehicle.

The figure shows a typical behaviour over a week, but the charging patterns change due to weather and unpredictable occurrences during the day. Figure 11 shows an example of a daily charging routine for the EV fleet.

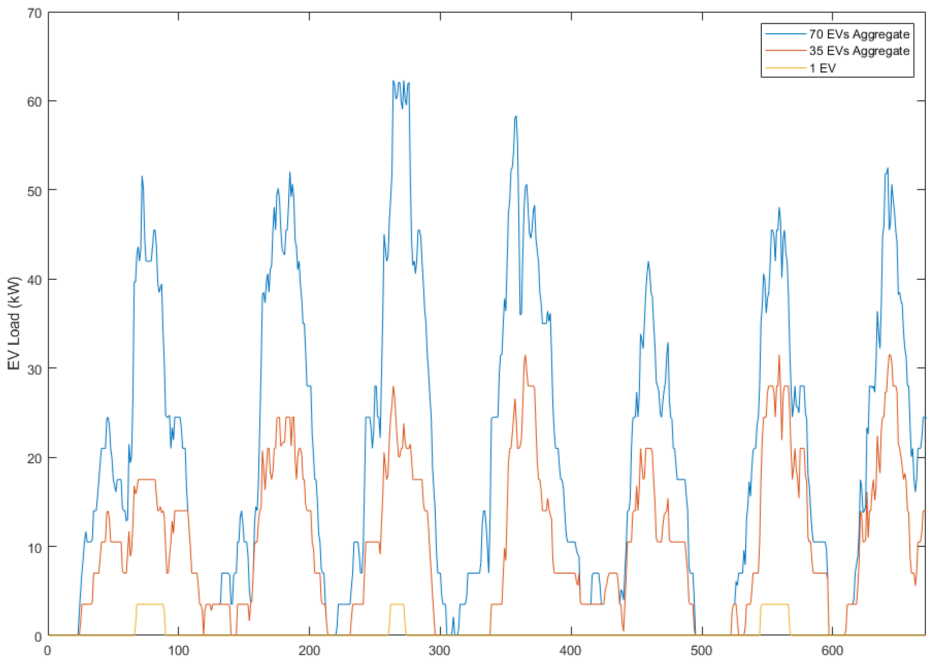

Figure 10 - Weekly EV load for different aggregates

Since the analysed grid is a medium voltage one and all the buses work at 4.8 kV, an aggregate of EVs must be created and used as an additional load to the cabinets. Thus, it is required to determine the number of profiles to aggregate at each bus.

This parameter will be calculated, similarly to the PV generation, by setting the EV penetration and solving for the total number of EVs, N_EV.

$$Pen_{EV} = \frac{\sum_{i}^{N\_EV} P_{max,EV,i}}{\sqrt{\sum_{i=1}^{N_{loads}} ({P_i}^2 + {Q_i}^2)}} \tag{33}$$

Since the maximum charging power of each EV is constant at 3.5 kW, the equation can be rewritten as a function of the number of aggregated EV profiles

$$Pen_{EV} = \frac{Pmax, EV \cdot N_{EV}}{\sqrt{\sum_{i=1}^{N_{loads}} ({P_i}^2 + {Q_i}^2)}} \tag{34}$$

Solving for the total number of EVs on the grid yields

$$N_{EV} = \frac{Pen_{EV}}{P_{max,EV}} \sqrt{\sum_{i=1}^{N_{loads}} ({P_i}^2 + {Q_i}^2)} \tag{35}$$

Not all the buses have the same base load, so we need to split the total number of EVs according to the nominal active power consumption at each bus

$$\boldsymbol{N_{EV}} = \boldsymbol{W} \cdot N_{EV} \tag{36}$$

where **N_EV** is the matrix featuring the number of vehicles at each bus which also has a load and **W** is a weighing matrix calculated as the percentage of apparent load power at each bus over the total consumption of the grid

$$\boldsymbol{W} = \begin{bmatrix} S_{Bus1}/Stot \\ \cdots \\ S_{Bus37}/Stot \end{bmatrix} \tag{34}$$

The last step was done to avoid having buses where the number of aggregated EVs and the active load power are unbalanced.

8.5 Battery Systems

The batteries are implemented by using the OpenDSS native model and delta connected to each bus where there is a load. This assumption prevents the possibility of having batteries in buses without a load, since an optimization of the placement would then be needed, which is not the scope of this report.

The discharging and charging powers follow the control described in the next chapter and try to store the PV overproduction and support the load consumption.

The storage systems are all connected in 4.8 kV and have a reserve SOC of 10%, while the storage size was estimated by assuming that the grid should be autonomous for 4 hours if the SOC of each battery is 50% and the batteries are discharged at nominal load active power. The hours of autonomy of the grid are

$$N_{aut} = \frac{Cap_{BESS,tot} \cdot SOC}{\sum_{i=1}^{N_{loads}} P_i} \tag{35}$$

Solving for the total storage capacity yields

$$Cap_{BESS,tot} = \frac{N_{aut} \cdot \sum_{i=1}^{N_{loads}} P_i}{SOC} \tag{36}$$

which then allows us to estimate the storage capacity installed on each bus as

$$\boldsymbol{Cap_{BESS}} = Cap_{BESS,grid} \cdot \frac{\mathbf{P}}{\sum_{i=1}^{N_{loads}} P_i} \tag{37}$$

Where

$$\boldsymbol{Cap_{BESS}} = \begin{bmatrix} Cap_{BESS,Bus1} \\ \cdots \\ Cap_{BESS,Bus37} \end{bmatrix} \tag{38}$$

And

$$\boldsymbol{P} = \begin{bmatrix} P_{Bus1} \\ \cdots \\ P_{Bus37} \end{bmatrix} \tag{39}$$

Table 4 - Values of battery capacity for each bus

Bus	kV	Conn.	kWh
701	4.8	delta	5040
712	4.8	delta	680
713	4.8	delta	680
714	4.8	delta	304
718	4.8	delta	680
720	4.8	delta	680
722	4.8	delta	1280
724	4.8	delta	336
725	4.8	delta	336
727	4.8	delta	336
728	4.8	delta	1008
729	4.8	delta	336
730	4.8	delta	680
731	4.8	delta	680
732	4.8	delta	336
733	4.8	delta	680
734	4.8	delta	336

735	4.8	delta	680
736	4.8	delta	336
737	4.8	delta	1120
738	4.8	delta	1008
740	4.8	delta	680
741	4.8	delta	336
742	4.8	delta	736
744	4.8	delta	336

8.6 Battery Control

A simplified controller has been designed to regulate the charging and discharging cycles. The process is controlled by the generation/consumption unbalance at the previous iteration, thus

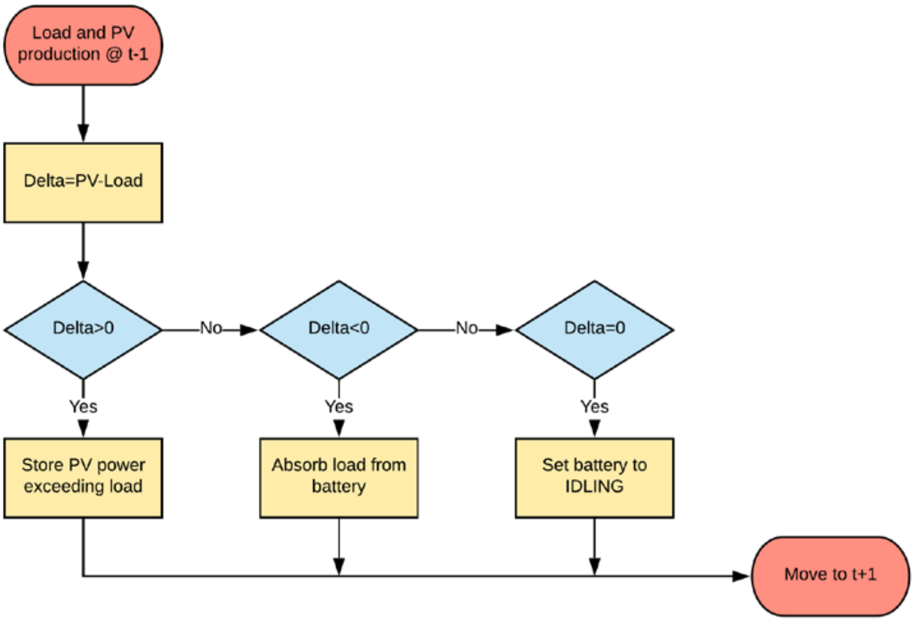

Figure 11 - Battery Control Strategy

helping the system to keep the voltage inside the 0.95 – 1.05 p.u. boundaries. The PV production is stored in case it's not needed while the load is taken from the battery if the SOC is higher than the reserve threshold.

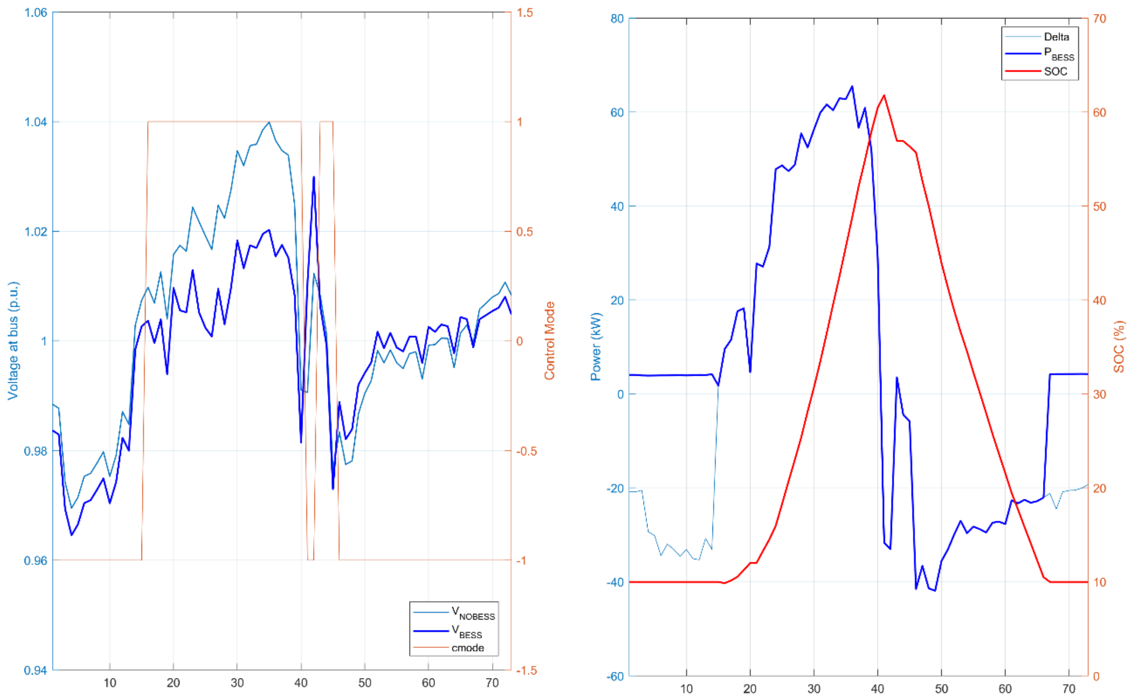

Figure 12 - An example of how the control of the battery works.

Figure 13 shows the control of the battery and its effects on the power flow. The bus is one of the furthest from the transformer but not the most distant, thus the effects of the loads and PV production on the voltage levels are much more noticeable than for a bus which is very close to the transformer. The most distant bus was not chosen because it is influenced too much by the downstream ones.

The control mode (cmode) is just a code to show what the battery is told to do: 1=charging/-1=discharging/0=idle.

From left to right, the battery is trying to discharge to support the load but the state of charge (SOC) is at the reserve level, thus the battery idles. The voltage results at the same level as in the case without the batteries, slightly lower because of the effects of the other buses on the analysed one.

The control lowers the voltage levels when the PV production is more than the load (Delta curve is >0 on the right plot) by charging the battery int eh central hours of the day.

Conversely, the loads are firstly satisfied by discharging the battery, which means that the voltage results to be slightly higher than the “no storage” solution (see plot to the left). That happens in the afternoon. The SOC of the battery raises and lowers accordingly, as we see on the right plot in red.

9 Simulation results for a test distribution grid

The different combinations of PV, EV and batteries were compared based on different indicators:

1. Under/Overvoltages count at each bus
2. Voltage deviations at each bus
3. Transformer overloads
4. Transformer under/overvoltages
5. Lines overload

The analysis of the results will present at first each single case, then the mitigation through storage. Only the most relevant results will be showcased.

9.1 Static Power Flow

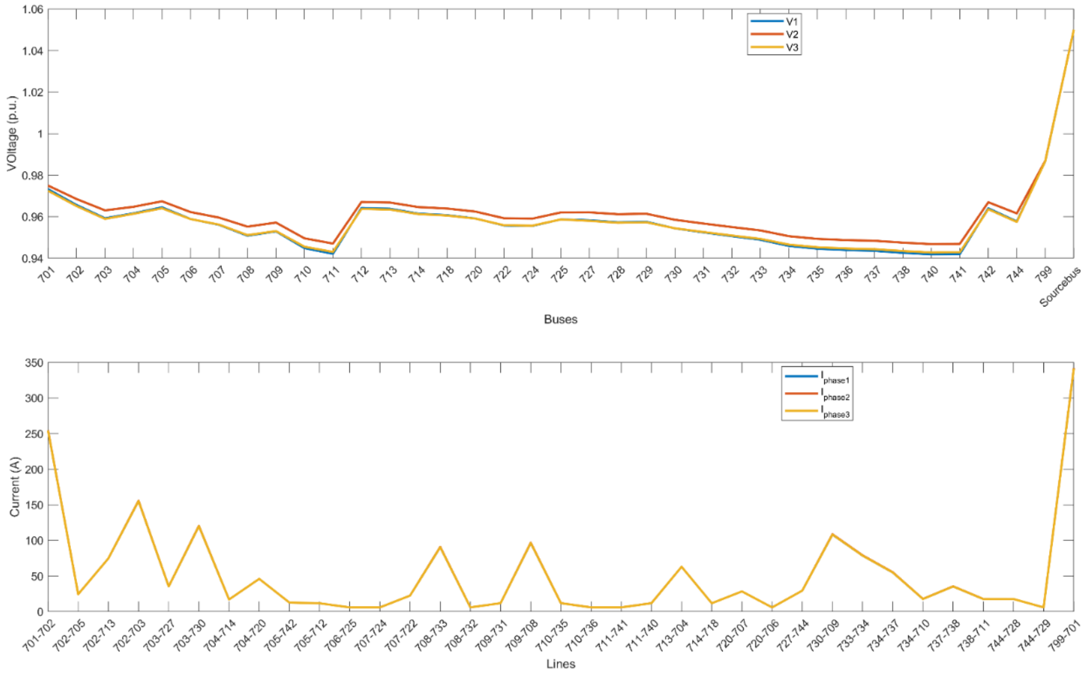

Figure 13 - Voltages and currents for a Steady State simulation at each bus on the 3 phases

As we can see in Figure 14, the voltage shows little to no variation among the phases, but a significant undervoltage situation is shown at some of the buses. This is because the 37 buses grid is designed as a sample case for unbalanced loads on MV grids.

In any case, this behaviour is highlighted by the fact that all the loads in static mode are supposed to be consuming their nominal power, which is of course unrealistic because of the non-contemporaneity in the load patterns. Thus, a sizeable change is expected in the QSS case.

It should be also noted that the buses which are subject to the lowest voltages are number 741 and 711, which happen to be the furthest from the substation (see Figure 10).

The currents also show a very high variation in magnitude, with peaks around the buses 799, 701 and 702, which are of course under high pressure because they convey the electricity to all the grid.

A final remark should be made regarding the phases: as the loads have been rebalanced and all the PVs are 3 phase, the electric parameters will show little to no variation among phase 1,2 and 3. Thus, from here onwards, the results be presented as an averaged value.

9.2 Static Power Flow + PV

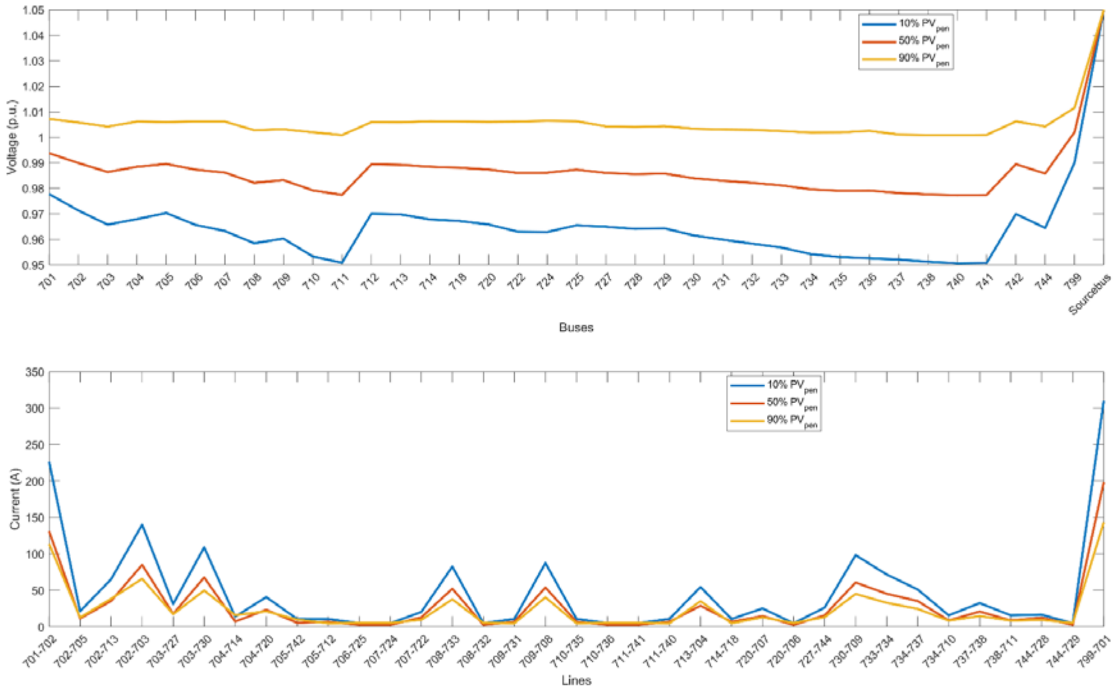

Figure 14 - Voltages and currents for a Steady State simulation with PV

The Steady State hypothesis with PV is even less realistic than with the loads only, as the panels are never going to produce their maximum power output for a whole year. Still, a variation of the PV penetration from 10 to 90% boosts the voltages from a situation where 2 buses are in undervoltage conditions (0.95 p.u. at buses 711 and 741) to a stable value of 1.01 p.u.

Another interesting remark is that the currents are showing a symmetrical behaviour compared to voltages. However, that comes as no surprise because the lower the voltage (10% PV penetration), the higher the current, since the loads are constant PQ.

Once more, the lines presenting the highest current values are detected along the main feeder connecting the transformer to the secondary branches.

9.3 QSS Power Flow (Loads Only)

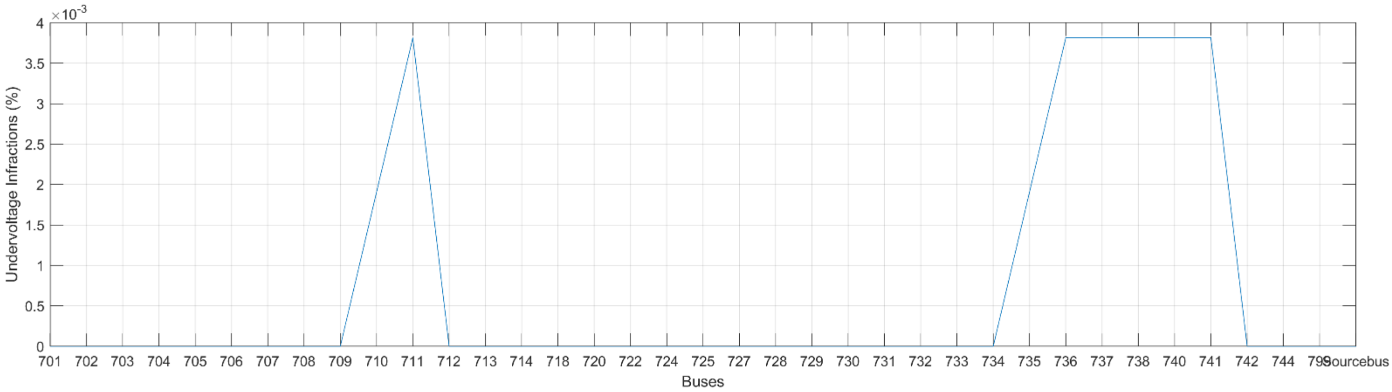

Figure 15 - Undervoltage Infractions for each bus of the grid.

While there are no overvoltage violations, the highest number of undervoltages results at buses 711 and 736-741, even if very small ($3.75 \cdot 10^{-3}$ % equals to 30 time units per year). The grid is thus very stable under QSS conditions.

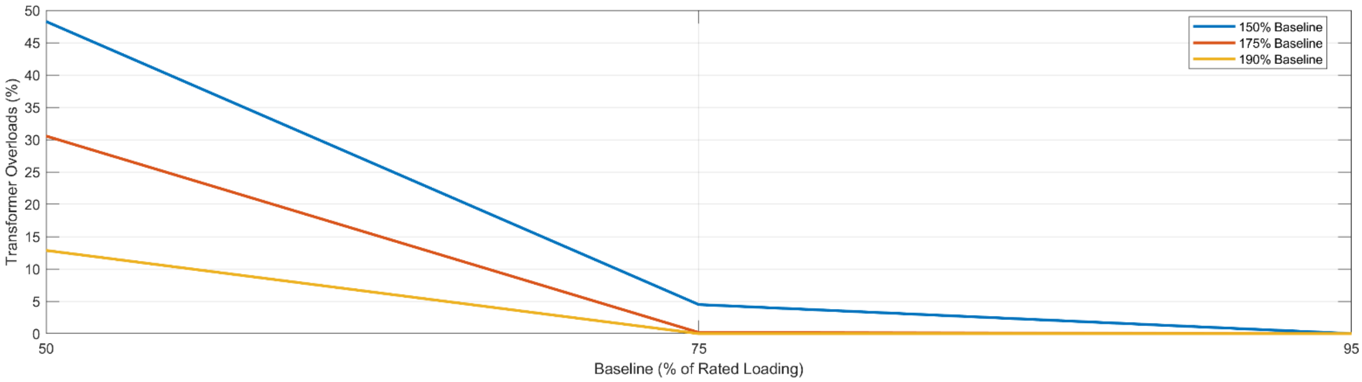

Figure 16 - Transformer Overloads for the 3 baseline ratings.

Transformer overloads were considered for 3 different scenarios in which the baseline percentage is changed from 50% of the rated power (MVA) to 95%. The three plots represent a 150 to 190% violation of the baseline. Normally the results would be calculated in number of consecutive minutes of overload but since the timestep is 15 minutes this is not possible. Of course the 190% overload is the most difficult one to reach, thus the number of occurrences is lower. As far as the voltage at the transformer is concerned, no violations are highlighted

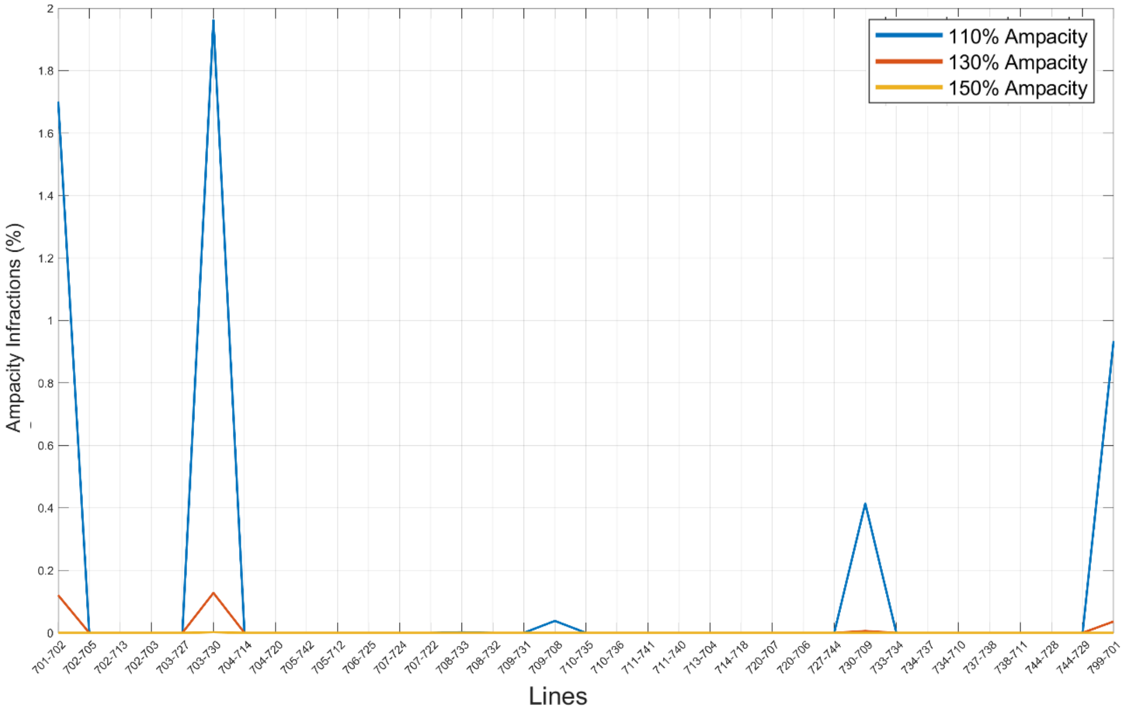

Figure 17 - Ampacity violations along the lines.

Another important aspect is the analysis of the ampacity violations along the lines, as shown in Figure 18. The lines connecting bus 799 to 709 are the most stressed ones, due all the branches feeding lateral buses.

It is also notable that 10% violations of the ampacity are much more frequent because the power requirement is lower, thus more likely to be met.

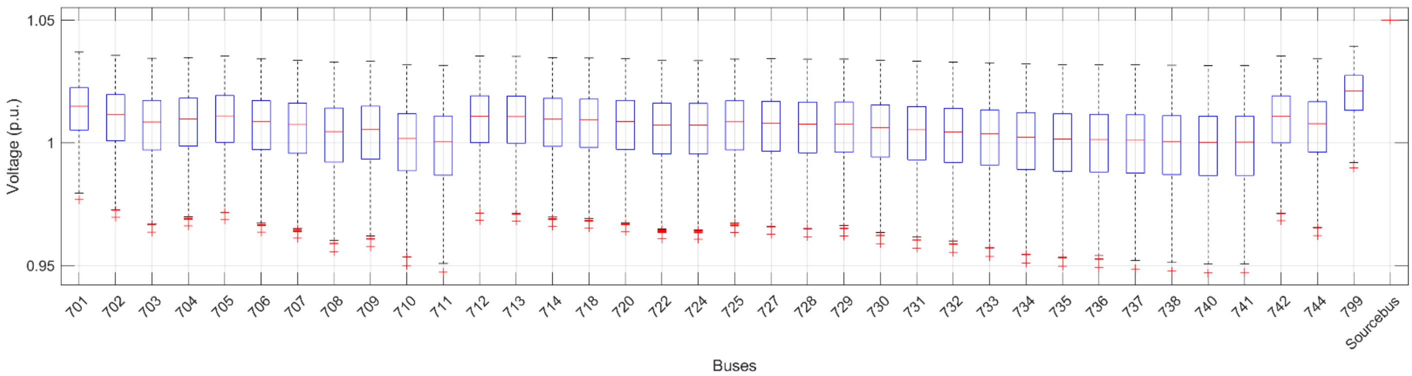

Figure 18 - Boxplot of the voltages for each bus of the grid.

The last analysis was performed on the voltage at the buses and the boxplots highlight a median value close to 1.01 p.u. and two separate subgroups of buses: the first from bus 701 to 707 and from 712 to 727, which we can consider as the least influenced by the loads. The second one includes all the other buses, notably the most distant ones, featuring a lower median (around 1 p.u.). The distance between the 25th and the 75th percentiles is also increasing as the median value decreases from left to right in Figure 19. Indeed, the increased distance from the source bus affects the voltage magnitudes during the whole simulation time, thus the range of the values is larger and the dispersion increases.

9.4 QSS Power Flow + PV

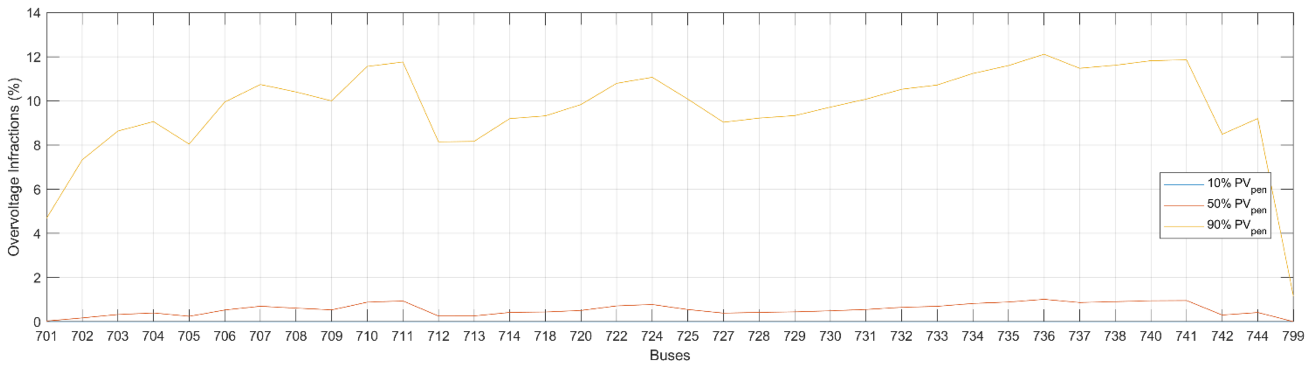

Figure 19 - Overvoltage infractions on all the buses of the grid when PV is installed.

The undervoltages show no difference with respect to the QSS with the loads only while the overvoltages are present throughout all the grid, especially when the PV penetration reaches 90%.

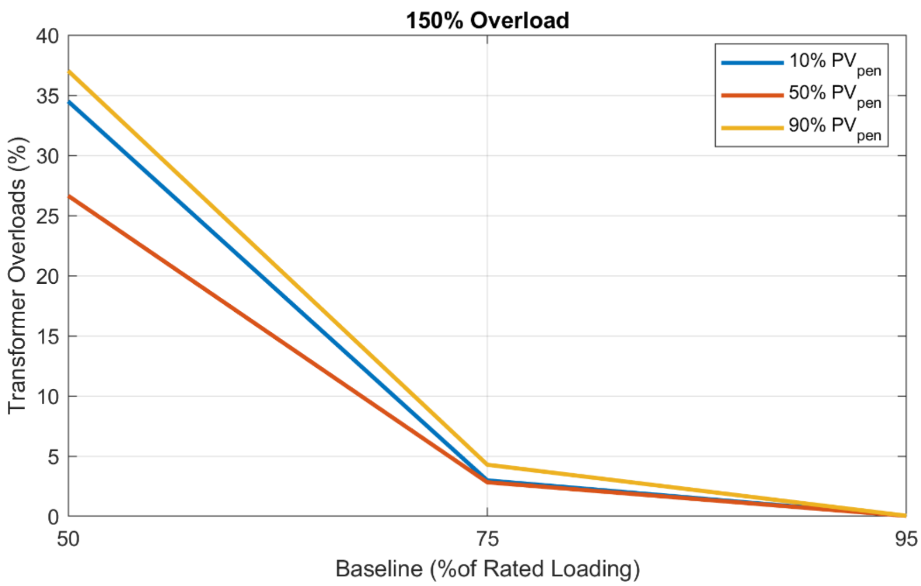

Figure 20 - Transformer overloads with PV: the baseline is trespassed by 50% of its value.

In this scenario, Figure 21 shows overload violations at the transformer. It must be noted that increasing the PV penetration is not always beneficial to the problem, since 90% Pen produces more overloads, in the form of reverse currents, than 10% penetration. Compared to the “loads only” case, the situation is better when the PV penetration is around 10%, producing a sizeable decrease of the infractions, around 15% (5256 time units).

As the baseline increases to 75%, the case with PV is slightly worse (5% more infractions), while at 90% both cases reach 0%. The most important takeaway is that the PV penetration should not be oversized, otherwise overloads and overvoltage problems will always be present but due to reverse flows.

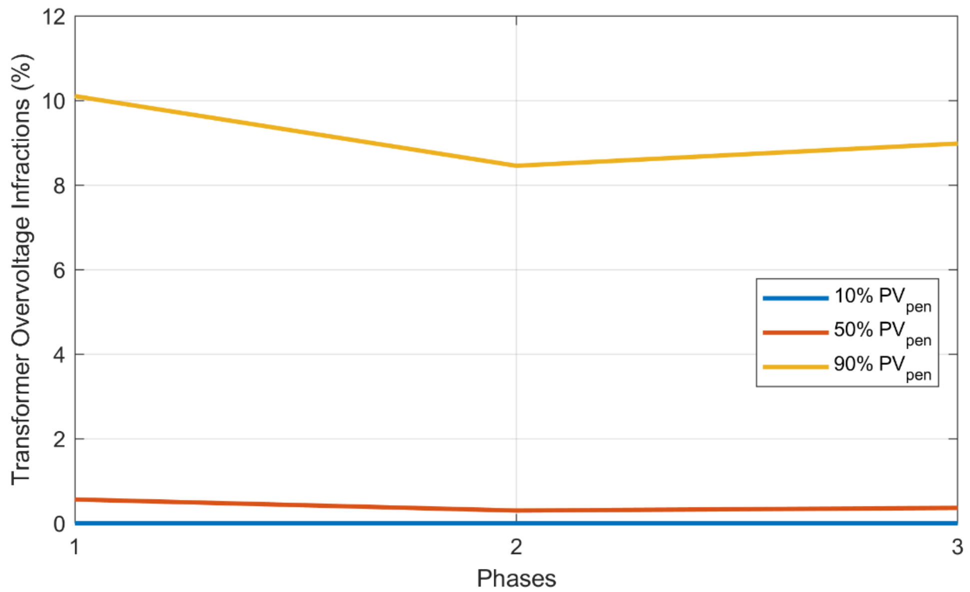

Figure 22 - Overvoltage infractions at the transformer when PV is installed.

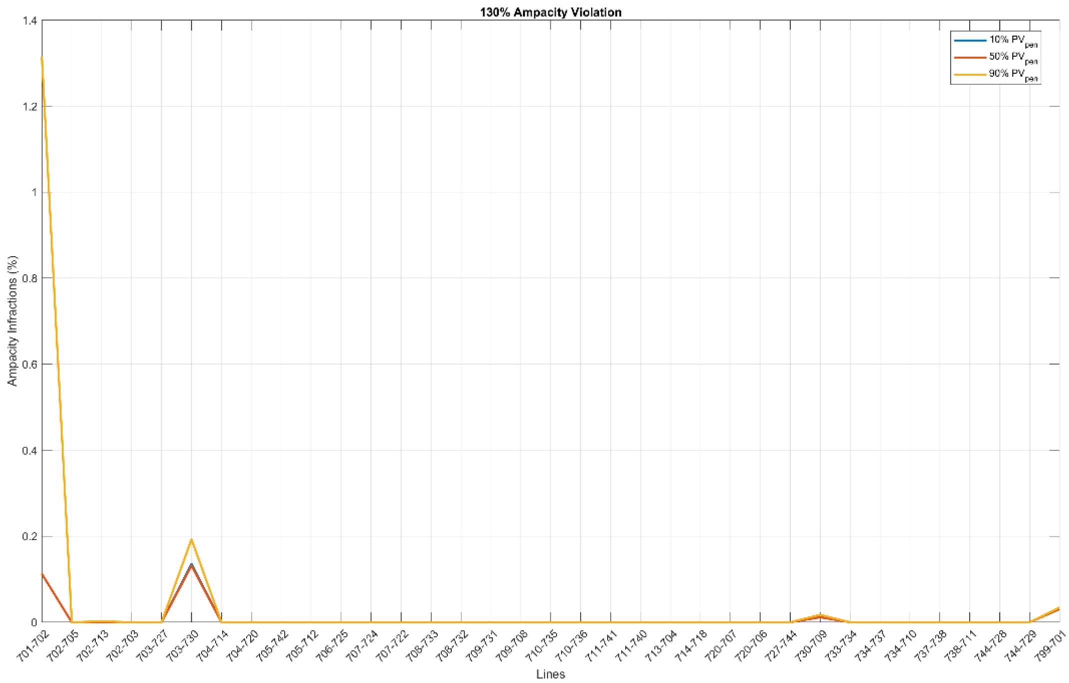

Figure 21 - Ampacity infractions when PV is installed.

In this case scenario there are no undervoltages but, as Figure 23 shows, overvoltages are present on all the phases when PV penetration reaches 90%. The behaviour is different from the overloads in Figure 21 because this time a higher penetration always causes a higher voltage infractions number.

The ampacity violations along the lines (Figure 22) show a very different behaviour compared to the “loads only” scenario. The peak is around 1.3%, and is located at the line between bus 701 and 702, as for the “loads only”, whereas line 703-730 has no infractions. The mentioned peak happens because that line collects all the PV production from the grid and the infractions are due to the simultaneity of the generation much more than the loads consumption.

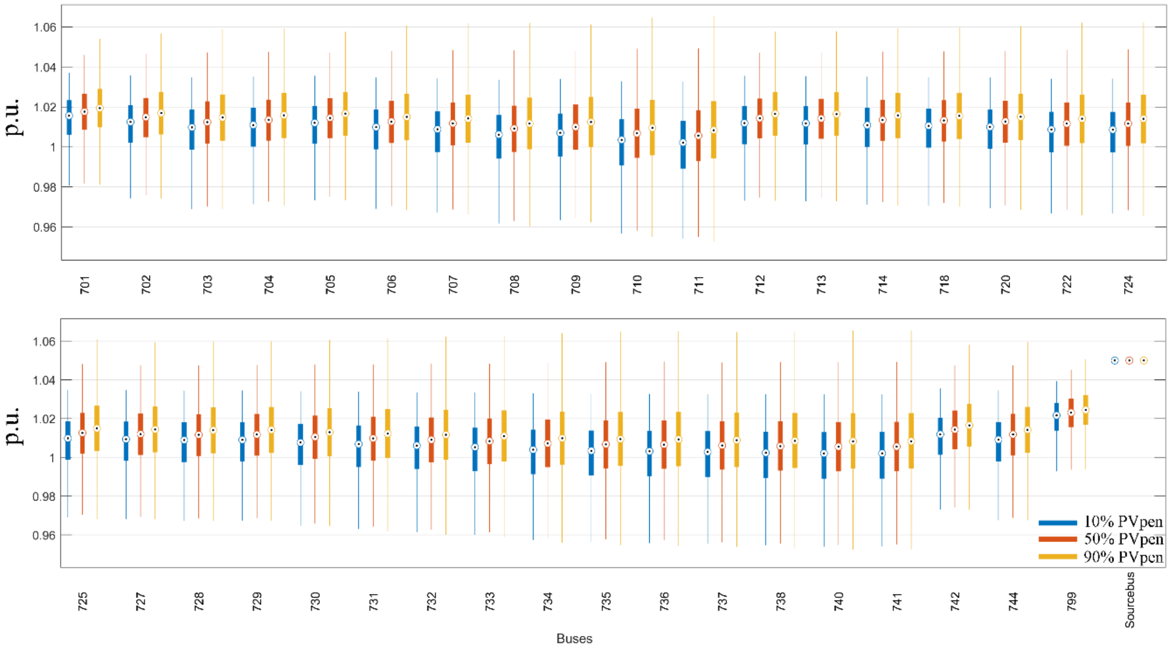

Figure 23 - Boxplots of the voltages for all the buses when PV is installed.

The voltage levels at the buses (Figure 24) show a greater dispersion compared to the QSS “loads only” when the penetration gets to 50 and 90% and generally the median is higher than before, around 1.1 p.u. for all of the buses. Boosting the PV production from 10 to 90% PV penetration highlights a median increase of about 0.01 p.u.

9.5 QSS Power Flow + EV

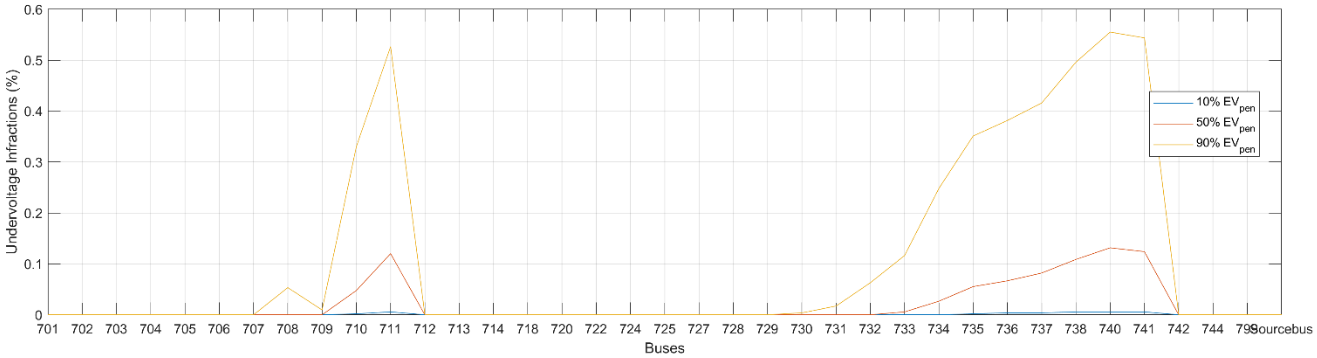

Figure 24 - Undervoltage infractions for each bus of the grid when the EV fleet is considered.

The undervoltage violations when EVs are included in the scenario (Figure 25) are more evident than the QSS "load only" but still they happen at the same buses, the most distant ones. The EV charging profiles have been aggregated to reproduce a fleet of PHEVs (Plug-In Hybrid Electric Vehicles).

The percentage of violations is around 0.5%, which means 175 time units out of 35040. Naturally, the highest EV penetration produces the highest number of infractions.

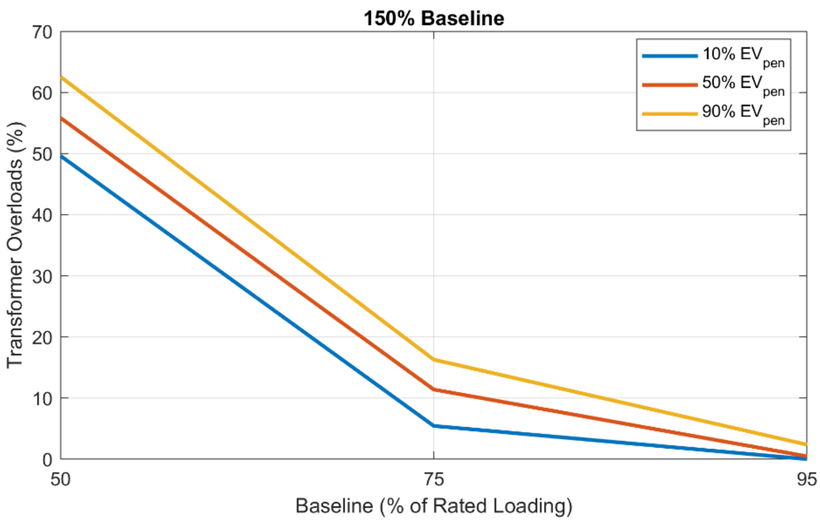

Figure 25 - Transformer overloads when the EV fleet is considered.

When analysing the transformer overloads for 150% of the baseline (Figure 26), it is possible to show that the infractions increase by around 15% when the EV penetration reaches 90%. As in the QSS "load only" case, there are no voltage infractions at the transformer.

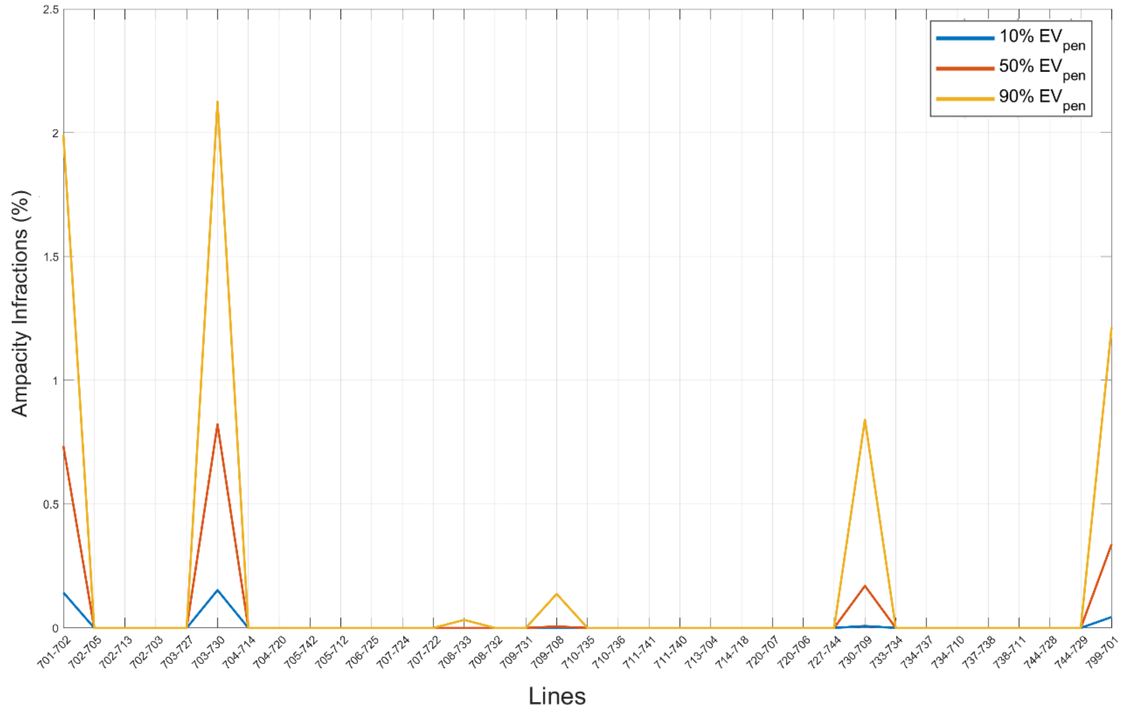

Figure 27 - 130% Ampacity infractions when the EV fleet is considered.

The situation from the ampacity violations side is shown in Figure 28. In the QSS "load only" case, when analysing the 130% Ampacity overload, the infractions number was peaking at 0.1% at the line between buses 703 and 730, while here 10% EV penetration peaks at 0.2% along the same line, so the results are consistent with the other scenarios. 90% EV penetration peaks at 2% violations, which equals 1114 time units out of 52416.

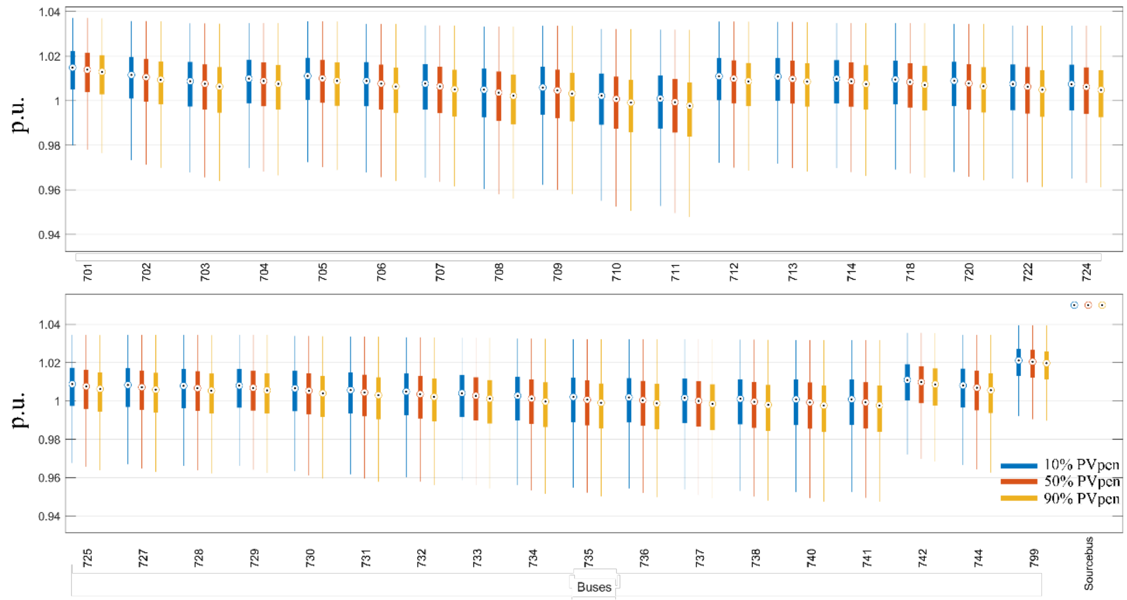

Figure 26 - Boxplots of the voltages at each bus of the grid when the EV fleet is considered.

The voltage boxplot in Figure 27 shows the impact of the electric vehicles on the grid: the median is around 1.01 p.u. for the first "group" of buses described in Figure 19 (Buses 701-707 and 712-

727). The most affected reach 1 p.u. instead. The distance between the 1st and 4th quartiles is comparable to the baseline scenario, so the effect of the EV fleet is a general reduction of the voltage magnitude at each bus. A secondary notable remark is that bus 799 is 0.05 p.u. lower with the EVs, due to all the other buses downstream.

9.6 QSS Power Flow + PV + EV

The first mitigation effect which can be analysed in OpenDSS is the passive voltage-lowering effect of the EV fleet charging, which partially compensates the PV generation voltage increase.

As the first plot of Figure 30 shows, the undervoltage occurrences are mostly concentrate on the same buses as before but comparing to Figure 25 we see almost no benefit from the installation of PV. This is probably because the undervoltage issues are concentrated in the morning and evening, when the PV production is typically lower. Since this type of mitigation is uncontrolled and based on the simultaneity between the electricity demand for EV charging and the PV production without the possibility to decouple them, the mitigation effects are weak.

This explanation is further confirmed by the analysis of the temporal distribution of the powers injected into the grid by the PV systems and consumed by the EVs, as in Figure 29. The picture shows that the generation is mostly concentrated between 8 a.m. and 7 p.m. whereas the consumption is mostly after 7 p.m. when people get home from work. The median also shows the PV production has a visible skewness towards higher values (75th percentile) before midday, then becomes symmetrical afterwards. The loads instead show a skewness towards the 25th percentile with a higher dispersion due to the non contemporaneity of the vehicle charging by the different users.

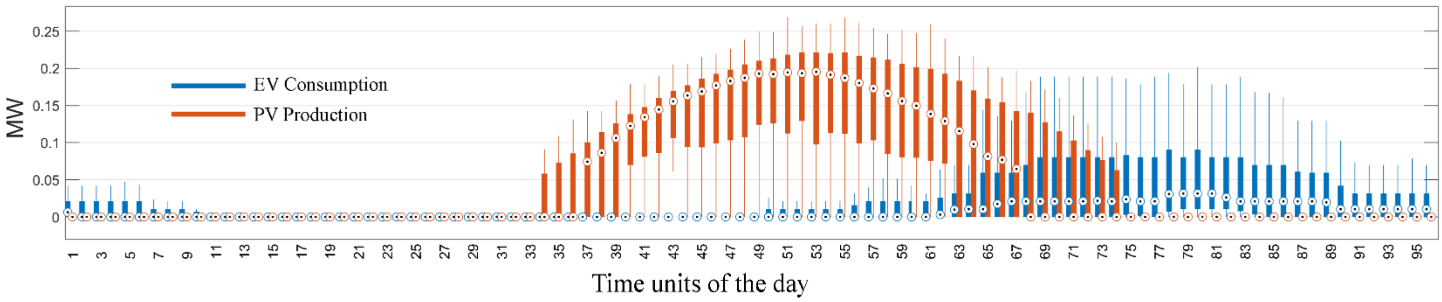

Figure 28 - Comparison between the PV production and the EV consumption for an average day.

The overvoltage occurrences are instead affected by introducing EVs as a mitigation. If we analyse the last plot of Figure 30, it is possible to note that when the PV penetration reaches 90% (the worst case for overvoltages) an increase from 10 to 90% EV penetration produces a reduction of around 2% of the overvoltage infractions.

The results are further confirmed if we consider that when the EV penetration is at its minimum (10%) the number of infractions is slightly lower than the “PV only” scenario with 90% PV penetration (Figure 20).

The transformer benefits from the consideration of both EVs and PV systems, as the overvoltages are present only after 50% PV penetration.

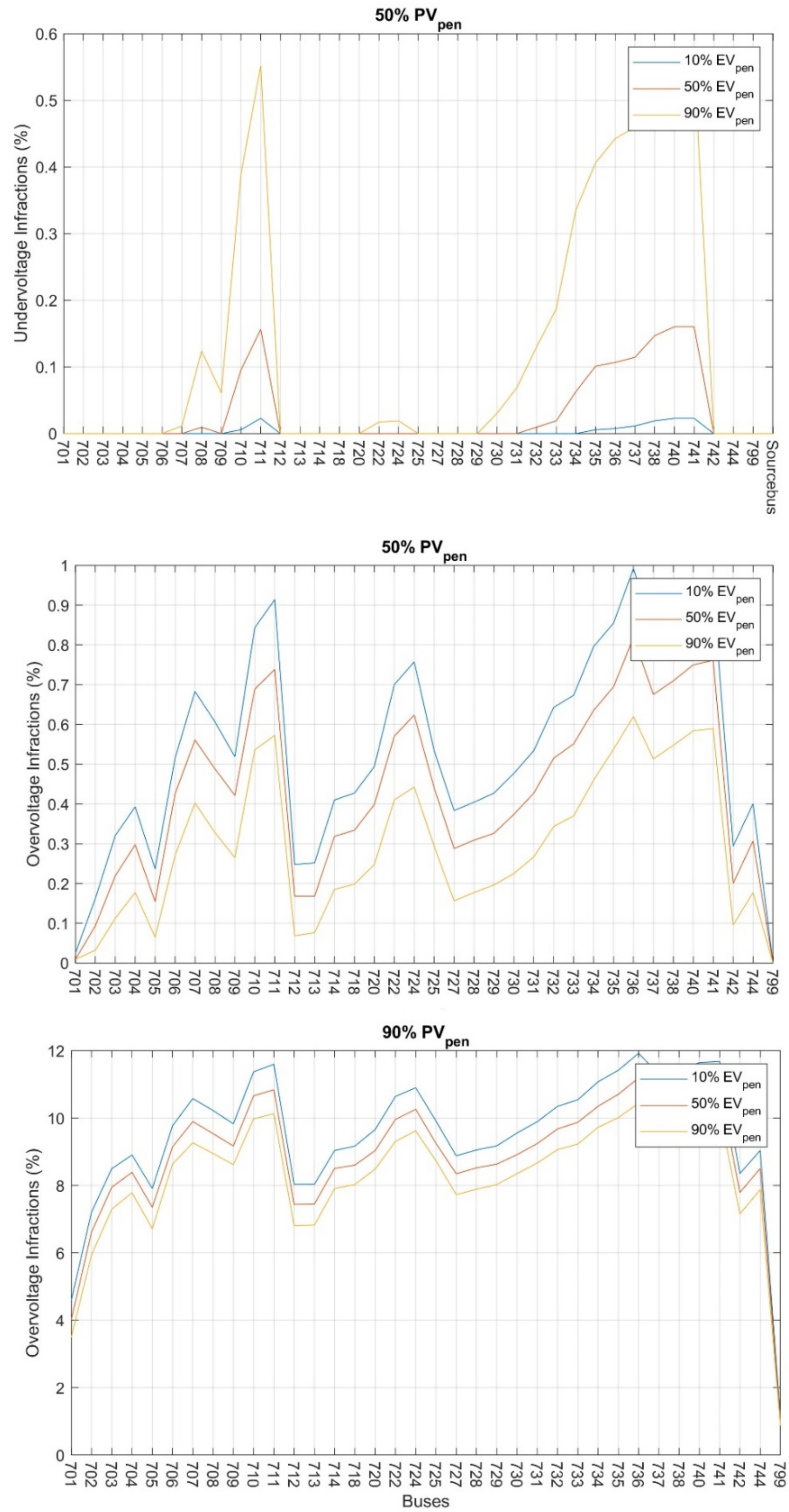

Figure 29 - Undervoltage (Top) and Overvoltage (Centre and Bottom) when both PV and EVs are considered.

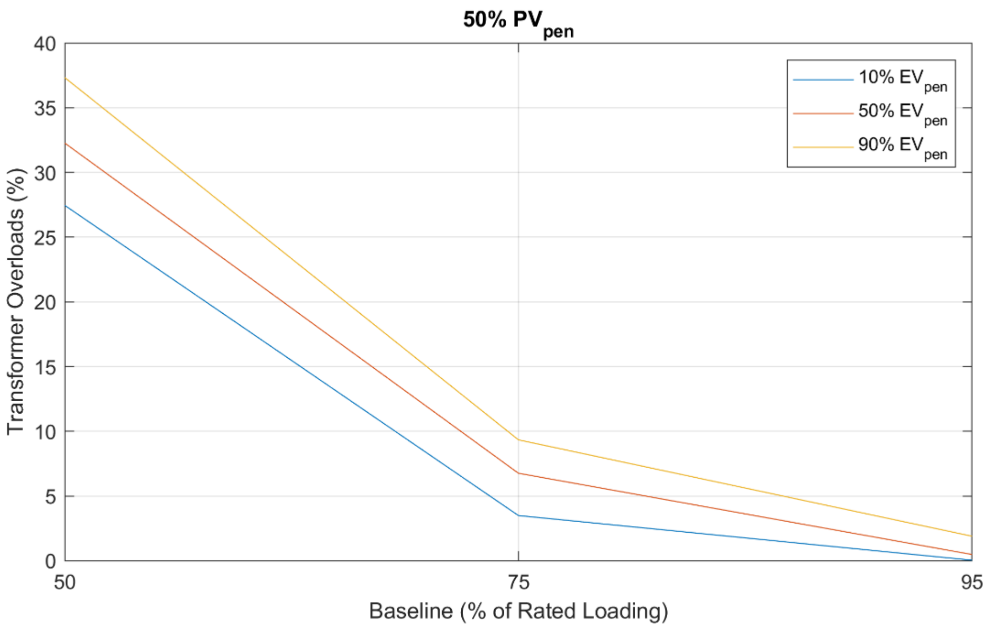

Figure 31 - Transformer overloads when both EVs and PV are considered.

As far as the overloads are concerned, Figure 32 highlights a great deal of improvement compared to Figure 26, a 50% EV penetration increase brings the overload occurrences from 55 to 32.5%, around 8059 time units out of 35040.

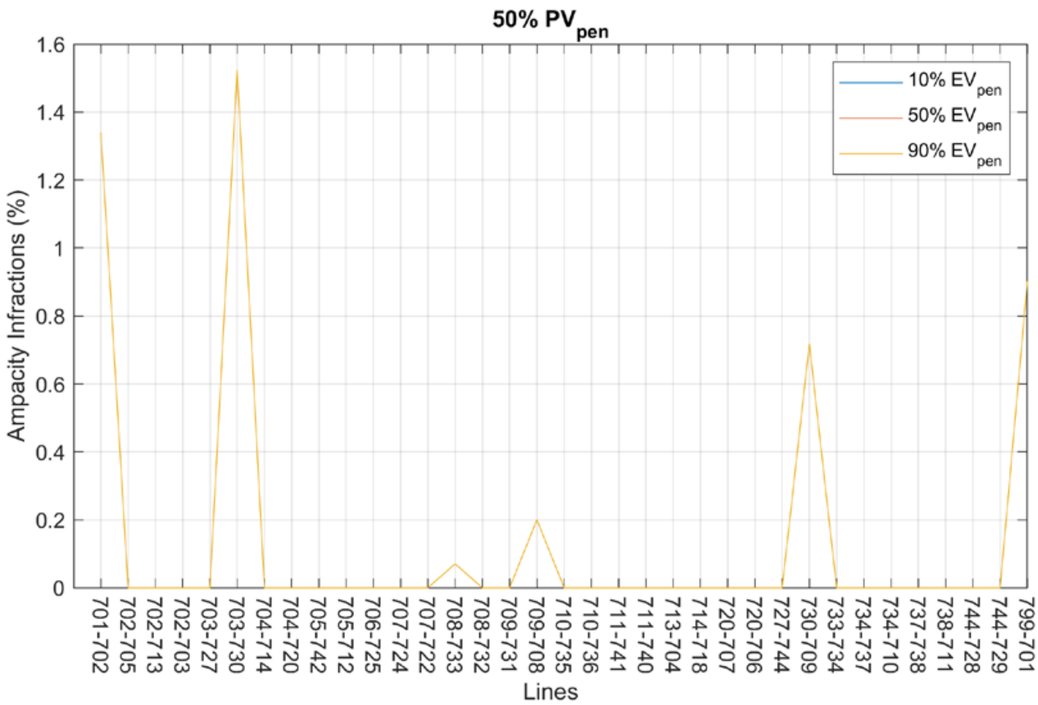

Figure 30 - Ampacity infractions when both EVs and PV are installed, 50% PV penetration.

Finally, as it was happening in Figure 28, the lines are overloaded mostly due to the load consumption and whenever a reverse flow is generated due to the PV systems producing during the central hours of the day, the lines experience overloading less frequently. Thus, Figure 33 shows a slight decrease due to the 50% PV penetration. The peaks are almost the same, around

1.5% for the lines between buses 703 and 730, but no infractions are detected for the 10 and 50% EV penetration scenarios.

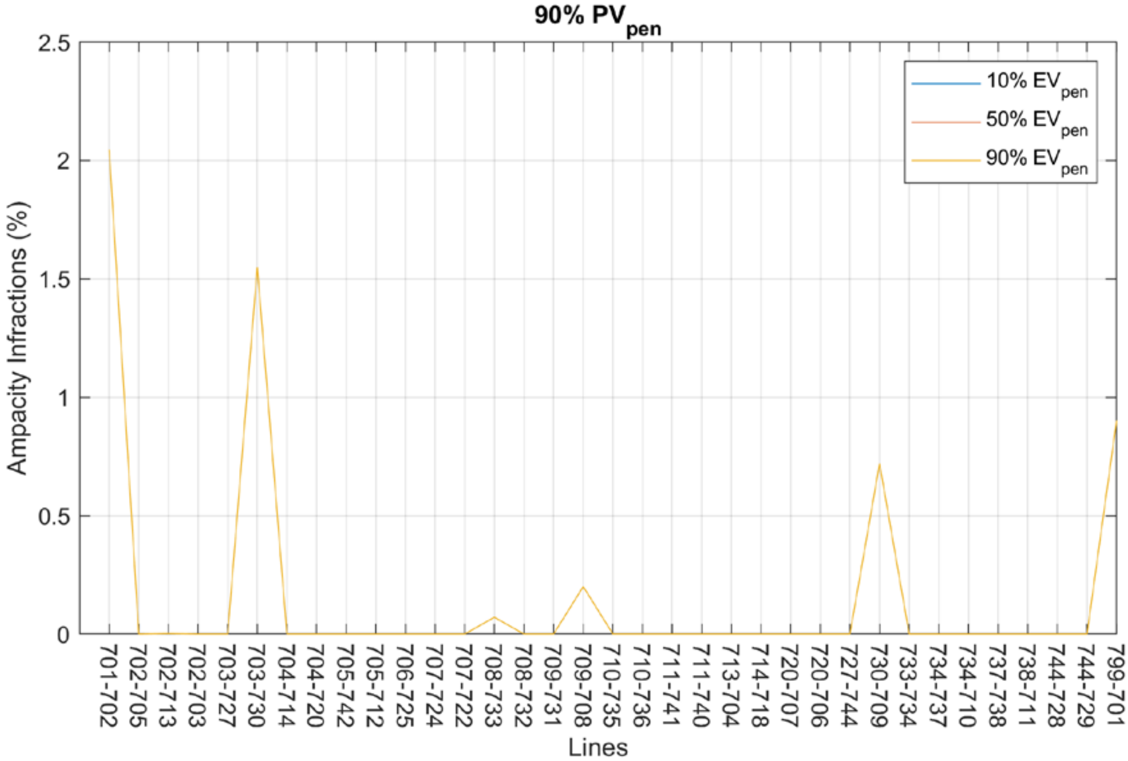

Figure 32 - Ampacity infractions when both EVs and PVs are installed, 90% PV penetration.

A final remark is that the installation of high PV powers, as we see in Figure 33, produces more overloads than 50% PV (Figure 31). This is because, as explained before, overloads consider reverse flows too.

9.7 Battery Mitigation for PV

Finally, battery storage was implemented to assess the benefits of production and demand decoupling on the electric parameters we analysed.

The voltage infractions as in Figure 34 show a great deal of improvement compared to the case without batteries, most notably in the overvoltage section. The number of infractions decrease from 10% on average on all the buses to 3-6% with the batteries.

As far as the transformer is concerned (see Figure 36), the main changes are noticeable when the PV penetration is high: charging the batteries helps mitigating the loads effects on the voltages only when the PV power is enough to exploit the storage. Compared to Figure 21, the only scenario showing a decent reduction is the 90% PV penetration one, from 37.5 to 25% infractions.

The voltage at the transformer is also much more stable than with the PV only: the average infractions level lowers from 10 to 3.5%. The 50% penetration scenario doesn't present any overvoltage, in contrast with the one presented in Figure 23.

The ampacity infractions also greatly benefit from the introduction of storage, as the peak falls from 1.5 (Figure 35) to 0.125% (Figure 22). This shows that not only the voltage levels at the buses but also the lines benefit from lower reverse flows.

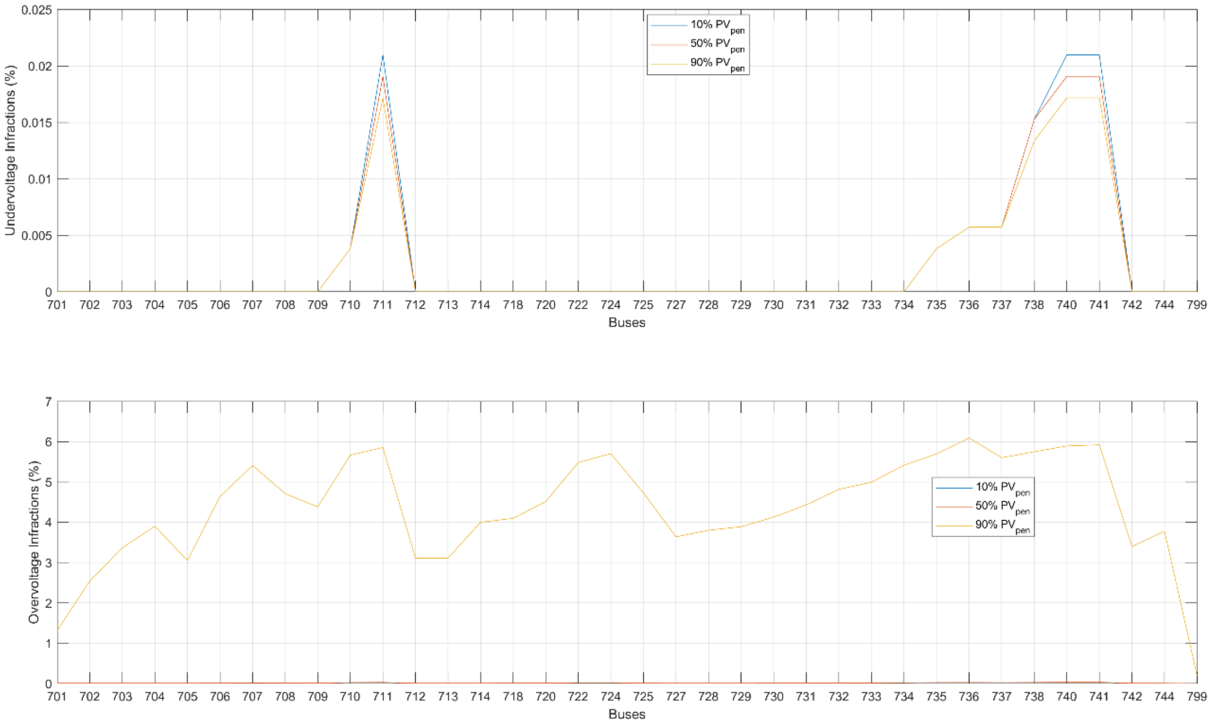

Figure 33 - Voltage infractions when PV and batteries are considered.

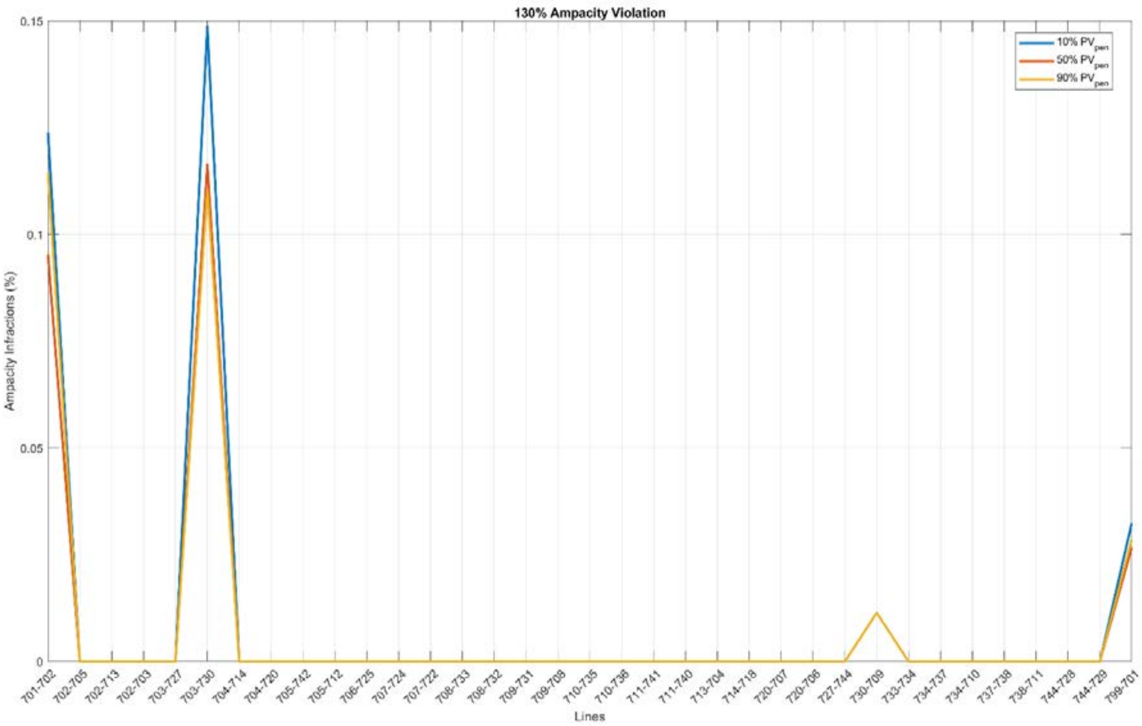

Figure 34 - Ampacity infractions when PV and batteries are considered.

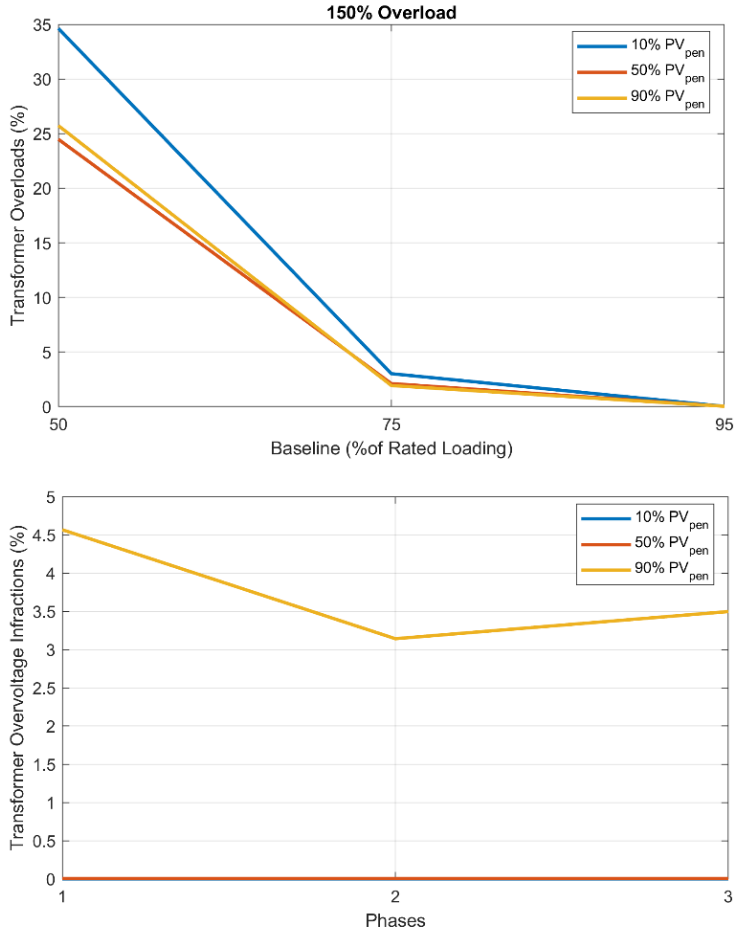

Figure 35 - Transformer overloads and Overvoltages when PV and batteries are considered.

9.8 Battery Mitigation for PV+EV

The same scenario was analysed for the PV+EV case by adding the same batteries. The undervoltage infractions are very similar as in the scenario without batteries, whereas the overvoltages show a great deal of improvement.

As we see in Figure 37, the overvoltages are reduced from a peak of 1 and 11% to of 0.035% as the penetration increases from 50 to 90%.

An interesting remark is that 90% EV penetration produces more overvoltages than the 10% case scenario. This is due to the control algorithm of the batteries, which helps sustaining the load up until the battery charge is depleted. Since the overall voltage levels are increasing due to the storage sustain, it is possible to see more overvoltage infractions even if the EV number increases. Thus, it is necessary to implement smart EV charging strategies, for example "vehicle to grid" or "vehicle to home".

The transformer is also less overloaded, but the greatest benefit is seen from the overvoltage standpoint at the substation, as we see in Figure 38. The overvoltage infractions, which before were around 0.55% are not a problem anymore. As for the buses, 90% EV penetration is slightly higher than the 50% case.

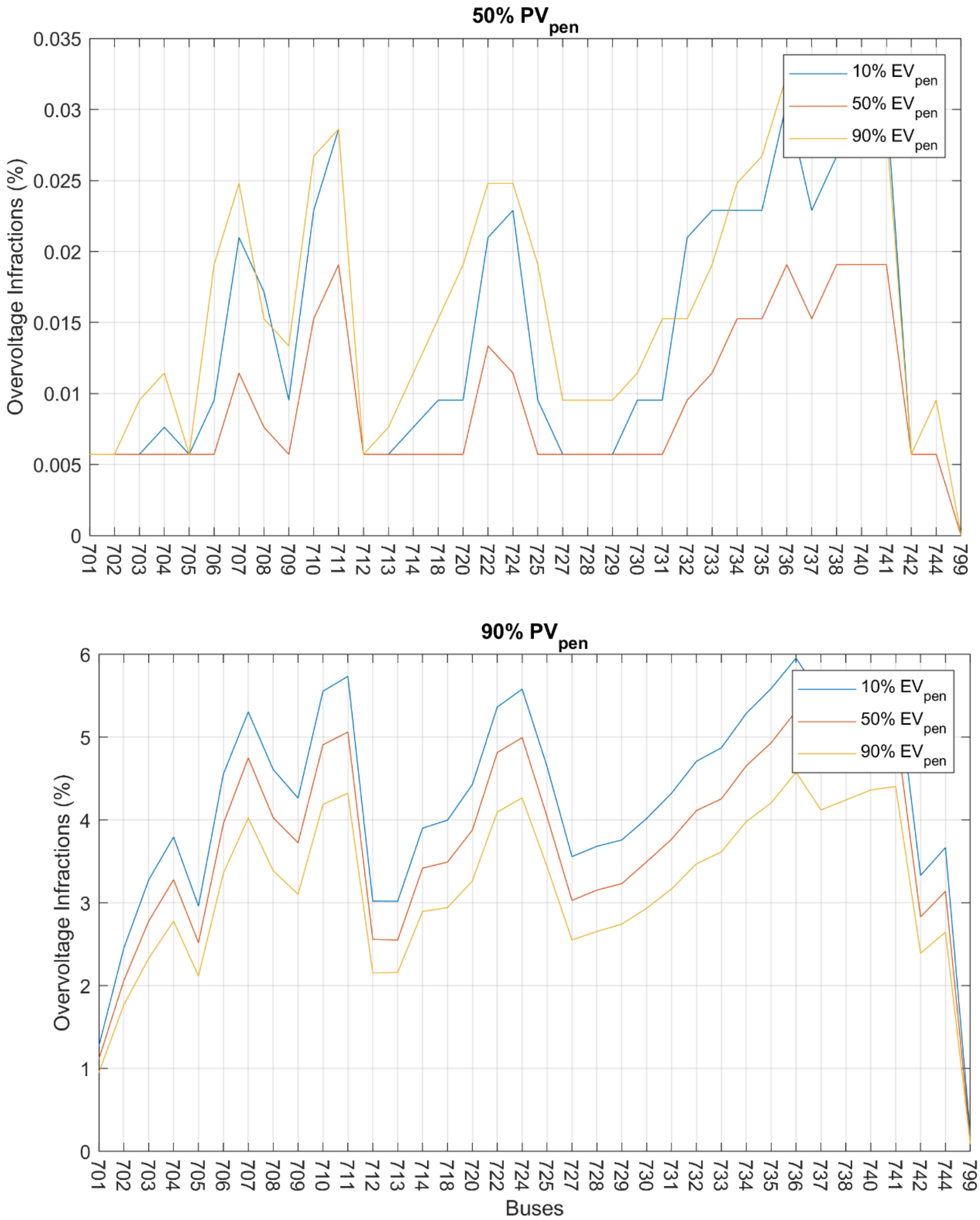

Figure 36 - Overvoltage along the buses of the grid when PVs, EVs and batteries are installed

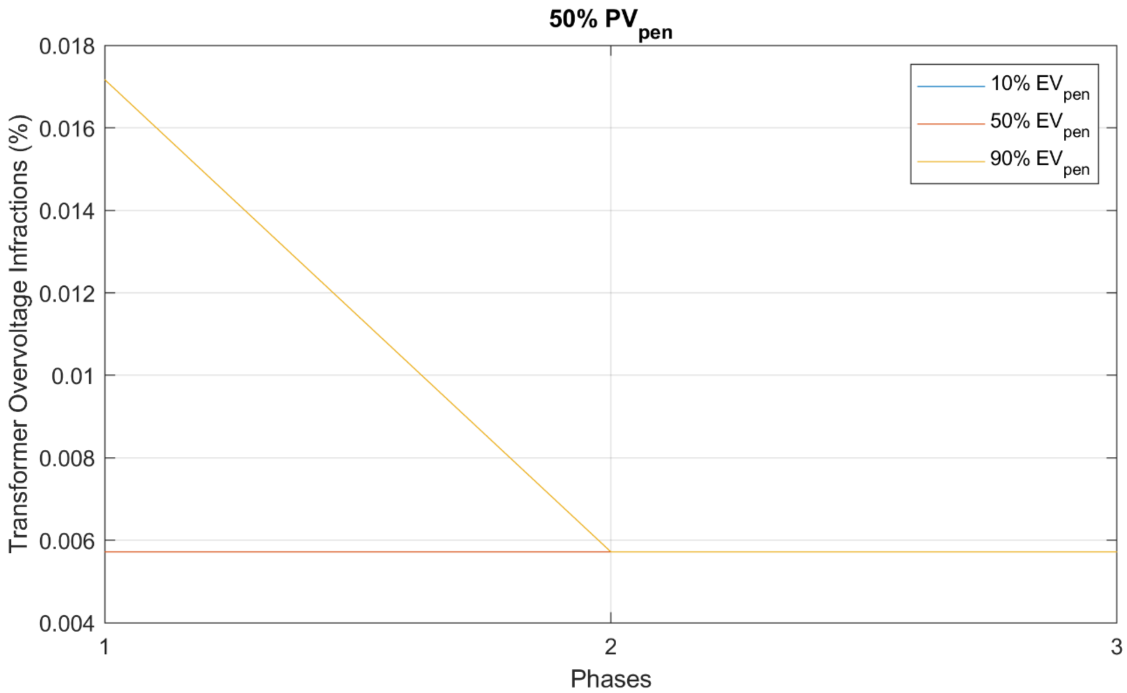

Figure 37 - Overvoltages at the transformer when PV, EVs and batteries are considered.

References

[1] X. Fang, S. Misra, G. Xue, and D. Yang, "Smart grid - The new and improved power grid: A survey," *IEEE Commun. Surv. Tutor.*, vol. 14, no. 4, pp. 944–980, 2012.

[2] W. H. Kersting, *Distribution System Modeling and Analysis*, 4th Edition. CRC Press.

[3] "A review of modelling tools for energy and electricity systems with large shares of variable renewables | Elsevier Enhanced Reader." [Online]. Available: https://reader.elsevier.com/reader/sd/pii/S1364032118305690?token=9FA90C048E925C957519CE3B81E1B13BD100DF97C9586A13BDB586B67CCA911F1CEF97A90678FB9C9582ADBD29188978. [Accessed: 13-Jun-2019].

[4] D. Connolly, H. Lund, B. V. Mathiesen, and M. Leahy, "A review of computer tools for analysing the integration of renewable energy into various energy systems," *Appl. Energy*, vol. 87, no. 4, pp. 1059–1082, Apr. 2010.

[5] T. Brown, J. Hörsch, and D. Schlachtberger, "PyPSA: Python for Power System Analysis," *J. Open Res. Softw.*, vol. 6, p. 4, Jan. 2018.

[6] L. Thurner *et al.*, "Pandapower - an Open Source Python Tool for Convenient Modeling, Analysis and Optimization of Electric Power Systems," pp. 1–8, 2017.

[7] T. Mai, J. Logan, N. Blair, P. Sullivan, and M. Bazilian, "RE-ASSUME: A Decision Maker's Guide to Evaluating Energy Scenarios, Modeling, and Assumptions," NREL/TP-6A20-58493, 1090954, Jun. 2013.

[8] "Caspoc Simulation & Animation for Power Electronics & Electric Drives." [Online]. Available: http://www.caspoc.com/products/caspoc/. [Accessed: 29-Jul-2019].

[9] "CYME - Software, Enhanced Substation Modeling." [Online]. Available: http://www.cyme.com/software/cymdistsub/. [Accessed: 29-Jul-2019].

[10] "Home - DIgSILENT." [Online]. Available: https://www.digsilent.de/en/. [Accessed: 29-Jul-2019].

[11] "GridLAB-D Simulation Software." [Online]. Available: https://www.gridlabd.org/. [Accessed: 29-Jul-2019].

[12] "Power system simulation | Power system Analysis | HYPERSIM." [Online]. Available: https://www.opal-rt.com/systems-hypersim/. [Accessed: 29-Jul-2019].

[13] "Ipsa 2 | IPSA Power." [Online]. Available: https://www.ipsa-power.com/?page_id=766. [Accessed: 29-Jul-2019].

[14] "MATPOWER – Free, open-source tools for electric power system simulation and optimization." [Online]. Available: https://matpower.org/. [Accessed: 29-Jul-2019].

[15] R. Dugan, "OpenDSS Introductory Training Level 1 Introduction," *Train. Mater.*, p. 85, 2009.

[16] F. Milano, "PSAT." [Online]. Available: http://faraday1.ucd.ie/psat.html. [Accessed: 29-Jul-2019].

[17] "RAPSim - Microgrid Simulator," *SourceForge*. [Online]. Available: https://sourceforge.net/projects/rapsim/. [Accessed: 29-Jul-2019].

[18] "SIMPOW." [Online]. Available: http://www.simpow.com/. [Accessed: 29-Jul-2019].

[19] "PHEV Home-Charging Model Based on Residential Activity Patterns - IEEE Journals & Magazine." [Online]. Available: https://ieeexplore.ieee.org/document/6422344. [Accessed: 22-Aug-2019].